Malaria Journal

RESEARCH

Open Access

Evaluating the potential of *Kalanchoe pinnata*, *Piper amalago amalago,* and other botanicals as economical insecticidal synergists against *Anopheles gambiae*

Sheena Francis[1,2*], William Irvine[1], Lucy Mackenzie-Impoinvil[3], Lucrecia Vizcaino[3], Rodolphe Poupardin[4,5], Audrey Lenhart[3], Mark J. I. Paine[5] and Rupika Delgoda[1]

Abstract

Background Synergists reduce insecticide metabolism in mosquitoes by competing with insecticides for the active sites of metabolic enzymes, such as cytochrome P450s (CYPs). This increases the availability of the insecticide at its specific target site. The combination of both insecticides and synergists increases the toxicity of the mixture. Given the demonstrated resistance to the classical insecticides in numerous *Anopheles* spp., the use of synergists is becoming increasingly pertinent. Tropical plants synthesize diverse phytochemicals, presenting a repository of potential synergists.

Methods Extracts prepared from medicinal plants found in Jamaica were screened against recombinant *Anopheles gambiae* CYP6M2 and CYP6P3, and *Anopheles funestus* CYP6P9a, CYPs associated with anopheline resistance to pyrethroids and several other insecticide classes. The toxicity of these extracts alone or as synergists, was evaluated using bottle bioassays with the insecticide permethrin. RNA sequencing and in silico modelling were used to determine the mode of action of the extracts.

Results Aqueous extracts of *Piper amalago* var. *amalago* inhibited CYP6P9a, CYP6M2, and CYP6P3 with IC_{50}s of 2.61 ± 0.17, 4.3 ± 0.42, and 5.84 ± 0.42 µg/ml, respectively, while extracts of *Kalanchoe pinnata*, inhibited CYP6M2 with an IC_{50} of 3.52 ± 0.68 µg/ml. Ethanol extracts of *P. amalago* var. *amalago* and *K. pinnata* displayed dose-dependent insecticidal activity against *An. gambiae*, with LD_{50}s of 368.42 and 282.37 ng/mosquito, respectively. Additionally, *An. gambiae* pretreated with *K. pinnata* (dose: 1.43 µg/mosquito) demonstrated increased susceptibility (83.19 ± 6.14%) to permethrin in a bottle bioassay at 30 min compared to the permethrin only treatment (0% mortality). RNA sequencing demonstrated gene modulation for CYP genes in anopheline mosquitoes exposed to 715 ng of ethanolic plant extract at 24 h. In silico modelling showed good binding affinity between CYPs and the plants' secondary metabolites.

Conclusion This study demonstrates that extracts from *P. amalago* var. *amalago* and *K. pinnata*, with inhibitory properties, IC_{50} < 6.95 µg/ml, against recombinant anopheline CYPs may be developed as natural synergists against anopheline mosquitoes. Novel synergists can help to overcome metabolic resistance to insecticides, which is increasingly reported in malaria vectors.

*Correspondence:
Sheena Francis
Sheena.francis02@uwimona.edu.jm
Full list of author information is available at the end of the article

Keywords Jamaican plants, *Kalanchoe (Bryophyllum) pinnata*, *Piper amalago* var. *amalago*, CYP, Mosquitoes, RNA-seq, Insecticide, Synergist

Graphical Abstract

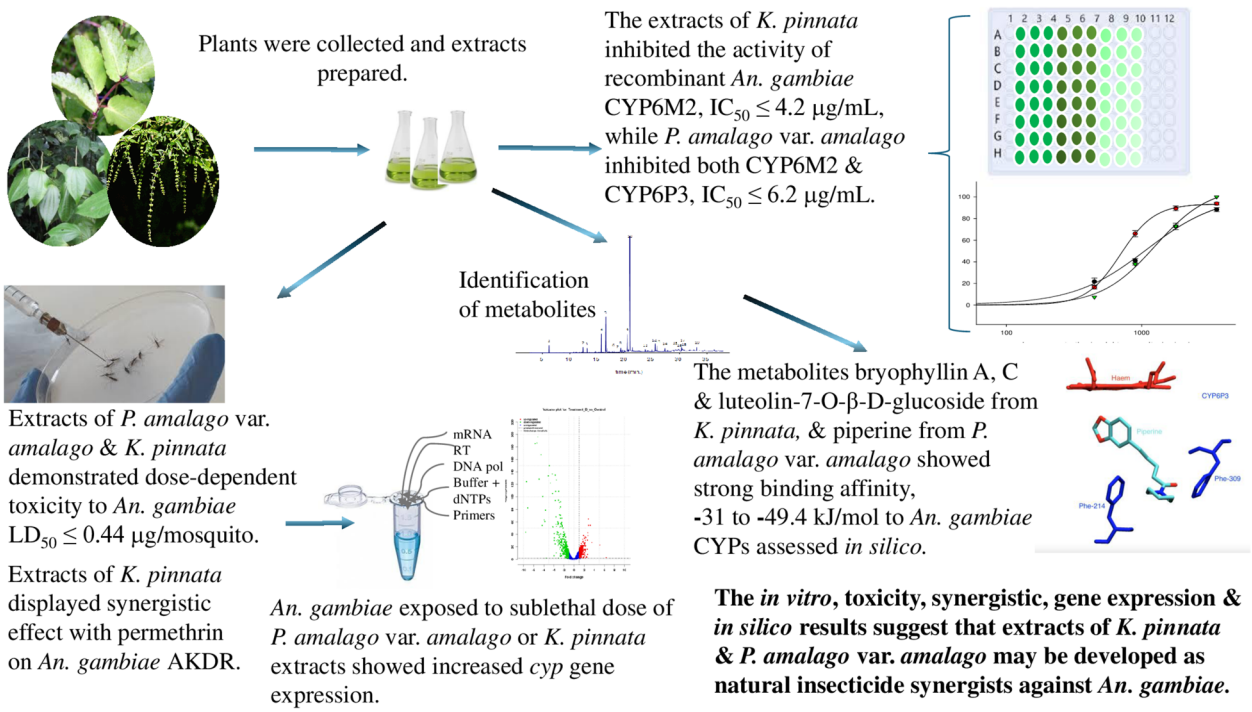

Background

The gains in malaria control by health authorities are consistently being challenged by widespread resistance of anopheline mosquito vectors to multiple classes of insecticides [1]. Changing climate trends are also expanding habitats for malaria and other tropical disease vectors [2]. Pyrethroids are the most commonly used insecticides for disease control as they are fast-acting, readily available, present relatively low mammalian toxicity, and are inexpensive. However, widespread use has led to high levels of pyrethroid resistance in mosquito vectors of malaria and other diseases [3, 4]. New tools to overcome insecticide resistance are urgently needed.

Mechanisms of resistance are complex and include insecticide avoidance, altered penetration, sequestration, target site alteration, or biodegradation. Metabolic resistance, associated with the biodegradation of xenobiotic compounds, is a common mechanism of resistance in mosquitoes caused by the overexpression of detoxification enzymes such as cytochrome P450s (CYPs), glutathione *S*-transferases (GSTs) and carboxy/cholinesterases (CCE) [5]. Of these, CYPs are the gene family primarily associated with resistance to pyrethroids and most other classes of insecticides used for vector control. In general, the evolution of consistently elevated levels of CYP gene expression in insects results in the rapid decomposition of insecticides, leading to a decrease in efficacy [5, 6]. However, compounds that can inhibit the catalytic activity of mosquito CYPs have the potential to reduce resistance caused by insecticide metabolism and reinstate susceptibility. Piperonyl butoxide (PBO), a broad-spectrum inhibitor of CYP activity, is commonly used in combination with pyrethroids as a synergist to increase their effectiveness against pyrethroid-resistant mosquitoes [7]. In 2017, the World Health Organization (WHO) recommended the use of pyrethroid–PBO combination bed nets for malaria control [8]. These have since proven more effective in reducing malaria cases than pyrethroid-only nets in areas of high pyrethroid resistance [9, 10]. Thus, identifying new compounds that inhibit CYP activity will increase the variety of synergists that can be developed to attenuate insecticide resistance, reducing the reliance on individual compounds that

might evolve resistance. Secondary metabolites of plants supply a large and diverse pool of compounds that block human metabolic enzymes by inhibiting their mode of action or serve as alternative substrates [11, 12]. As such, these metabolites may have application as synergists to overcome metabolic resistance in malaria vector populations known to overexpress CYPs. Work described in this paper was undertaken to explore the value of Caribbean biodiversity as insecticide synergists against anopheline mosquitoes, particularly routed through CYP inhibition.

Anopheles gambiae CYP6P3 and CYP6M2 and *Anopheles funestus* CYP6P9a are CYPs that metabolize pyrethroids and are frequently overexpressed in African populations of pyrethroid-resistant mosquitoes [13–15]. They are also associated with cross-resistance due to their broad substrate specificity and capacity to metabolize a wide range of different insecticide classes [16–18]. Heterologously expressed CYP6P3, CYP6M2, and CYP6P9a enzymes were used to screen extracts from native and non-native Jamaican plants with therapeutic or insecticidal properties, *Condea verticillata*, *Piper amalago* var. *amalago*, and *Kalanchoe pinnata*, to identify potential insecticide synergists and demonstrate their added toxic effect when used in combination with a pyrethroid insecticide. Further, in silico modelling was used to explore possible enzyme interactions with bryophyllin A, bryophyllin C, luteolin-7-*O*-β-D-glucoside in *Kalanchoe pinnata*, 2,3-diacetoxytormentic acid in *Condea verticillata*, and piperine in *Piper amalago* var. *amalago* (supplemental 1), compounds previously attributed to the insecticidal activities of these plants [19–22].

Methods

Reagents

Potassium phosphate, magnesium chloride, nicotinamide adenine dinucleotide phosphate ($NADP^+$), glucose-6-phosphate, glucose-6-phosphate dehydrogenase, deltamethrin (98%) dimethyl sulfoxide (DMSO) (99.9%), acetonitrile (99.8%), and piperine (97%) were purchased from Sigma-Aldrich (Gillingham, UK). Piperonyl butoxide (PBO; 90%; Fluka, Buchs, Switzerland), ethanol (99%), and acetone (99%) were purchased from Fisher Bioreagent (NJ, USA). Diethoxyfluorescein (DEF; 98.1%) was purchased from Cypex Ltd., (Dundee, UK), and permethrin (99%) was purchased from Chem Service Inc. (PA, USA).

Preparation of plant extracts

Eight aromatic plants widely used in Jamaica for their therapeutic or insecticidal properties were screened for their ability to inhibit heterologously expressed *An. funestus* and *An. gambiae* (sensu stricto) CYPs. Collected plant material was bench-dried and prepared according to previously developed and refined methods [23, 24]. Leaves and smaller woody material were finely crushed and prepared as infusions or decoctions as previously described [22, 25]. Briefly, 1 g of dried, finely ground material (leaf, stem) was infused in 100 ml of boiled deionized water for 15–20 min. Barks were decocted for 2 h and left to stand overnight. The resulting liquor was suction-filtered to remove suspended solids. The samples were lyophilized using a freeze-dryer (Labconco, MO, USA). The resulting solids were kept at − 20 °C until required and not subjected to more than two freeze–thaw cycles. *Bidens pilosa*, *Croton linearis*, *Condea verticillata*, and *Piper amalago* var. *amalago* were prepared from a leaf and stem infusion. *Bursera simaruba*, *Cinnamodendron corticosum*, and *Guazuma ulmifolia* were prepared from a bark decoction. *Kalanchoe pinnata*, a succulent plant, not native to Jamaica, was prepared from fresh leaves as a juice extract that was subsequently lyophilized. Voucher specimens of each plant sample were prepared and deposited in the herbarium at the University of the West Indies, Mona, Jamaica. Each specimen was identified by the botanist and herbarium curator, and given voucher numbers.

Ethanol extraction was conducted as follows: the aerial parts of each plant (*K. pinnata, C. verticillata*, and *P. amalago* var. *amalago*) were collected and left to air-dry over a 72-h period. The leaves and stem of each plant were pulverized and then submerged in 300 ml of analytical-grade ethanol. After the 72-h period, each extract was suction-filtered to separate plant particles from the extract. The extract was then concentrated via rotary evaporation (Büchi B-481, DE, USA), decanted and placed under a fume hood to remove excess solvent. The final mass of each extract was obtained.

In vitro mosquito CYP assays

Escherichia coli membranes expressing mosquito CYP co-expressed with CYP reductase were obtained from Cypex Ltd. (Dundee, UK): CYP6P9a from *An. funestus* and CYP6P3 and CYP6M2 from *An. gambiae* (sensu stricto) [16]. Diethoxyfluorescein (DEF), the fluorogenic substrate, was used to measure enzyme activity.

The Michaelis–Menten kinetics were initially calculated for each enzyme. These calculated values (CYP6P9a (40 pmol/ml; K_m 5 µM), CYP6P3 (40 pmol/ml; K_m 0.83 µM), and CYP6M2 (10 pmol/ml; K_m 1.66 µM) were employed for inhibitory activity from thereon. CYP assays were conducted on lyophilized plant extracts resuspended in either water or 0.1% final acetonitrile concentration per assay. DEF was dissolved in DMSO with a final concentration of 0.5%. A solvent

control was included to correct for any solvent effects across the dilution range. Single-point enzyme inhibition assays, conducted at 8.16 µg/ml plant extract, were initially conducted to determine whether the plant decoctions or infusions had an inhibitory effect on anopheline CYPs. Deltamethrin and PBO were used as standard controls to compare the inhibitory properties of the plant extracts. The procedure followed similar methods routinely conducted with human CYP enzymes [26, 27].

Extracts that demonstrated a percentage inhibition > 60% at 8.16 µg/ml were further assessed to determine IC_{50} values, the concentration at which 50% inhibition is observed. The enzyme assays were performed in triplicate using black 96-well plates (Thermo Labsystems, Basingstoke, UK), in 50 mM potassium phosphate buffer containing 5 mM $MgCl_2$, pH 7.4, with enzyme and substrate at the concentrations stated above while varying the concentration of the test compound. Reactions were preincubated at 37 °C for 5 min, while continuously shaken at 420 spm. The reactions were initiated by the addition of the NADPH-generating system consisting of $NADP^+$, glucose-6-phosphate, and glucose-6-phosphate dehydrogenase at final concentrations of 0.001 mM, 0.025 mM and 5 units/ml, respectively. The final reaction volume was 200 µL. The reactions were monitored at 485 nm excitation/530 nm emission using a fluorescence spectrophotometer with an incubator and shaker (Thermo Electron Varioskan, UK). IC_{50} values were calculated in SigmaPlot v. 10. (Systat Software Inc.).

Characterization of plant extracts by GC–MS and HPLC

The GC–MS system (Agilent 7820 A) was coupled to a mass selective detector (Agilent 5975 series; Agilent Technologies, CA, USA) with a Hewlett-Packard DB-5 ms column (60 m × 0.25 mm; 0.25 µm film thickness). Purified helium was used as the carrier gas with a flow rate of 1 ml/min. The temperature program employed was from 45 °C (1 °C/min) to 280 °C (2 °C/min). Injector and detector temperatures were maintained at 210 °C and 220 °C, respectively. The injection volume for the extract was 1 µl. Retention indices were directly obtained via the application of Kovats' procedure. The components of the extract were identified via a comparison of mass spectral data with those of the NIST17 library, as described in ref. [28].

Separation of the extract was undertaken using a stationary-phase HPLC (Agilent 1100 series, Agilent Technologies, CA, USA). The column used was C-18, with the solvents 75% acetonitrile: 25% water. The extract was standardized against piperine, a phytochemical identified with 99% confidence by the GC–MS analysis, that is known to contribute to the insecticidal properties of most Piperaceae [29–32].

Mosquito rearing

Extracts demonstrating strong inhibitory properties towards one or more anopheline CYPs in vitro were further assessed for their effect on *Anopheles* mosquitoes in vivo. Mosquitoes for the in vivo assays were obtained from the Malaria Research and Reference Reagent Resources center (MR4, CDC, Atlanta, GA, USA). They were maintained at a constant temperature of 27 ± 2 °C and 70 ± 10% humidity on a 14-h/10-h light/dark cycle (Environmental Specialties Incubator, Model ES 10–10 WR, NC, USA). Routinely, the larvae were maintained in trays (Bugdorm, Taiwan, L35 × W26 × H4.5 cm), with 350–500 ml of distilled water per 300 larvae. *An. gambiae* (G3 strain) larvae were fed a diet of 50–100 mg of ground koi pellets until pupation. *An. funestus* (Fumoz strain) larvae were fed 50–100 mg of ground koi pellets with the addition of 50 mg of powered *Spirulina* until pupation. Pupae were removed and transferred in cups to insect rearing cages (Bugdorm, Taiwan) per species. *Anopheles gambiae* (AKDR strain) pupae were obtained directly from MR4. Adult mosquitoes were provided 10% sucrose ad libitum.

Mosquito toxicity assay

Each prepared plant extract was resuspended in ethanol to give an initial stock solution (0.08–0.2 mg/µl), and then serially diluted (0–7.15 µg/µl) in ethanol. The resuspended extract was topically applied to the thorax of 3–5-day-old non-blood-fed adult *An. gambiae* (G3) or *An. funestus* (Fumoz) female mosquitoes ($n = 10$–30) following methods described in ref. [33]. Briefly, the female mosquitoes were anaesthetized on ice and 0.2 µl of the resuspended extract was applied to the dorsal thorax using a 700 series syringe and a PB600 repeating dispenser (Hamilton, NV, USA). The control treatment was applied with 0.2 µl of ethanol only. After treatment, mosquitoes were contained in paper cups and fed 10% sucrose solution. The mosquitoes were observed for 3 h to observe response to initial exposure. Mortality was recorded at 24 h under standard insectary conditions as previously described. Assays for each concentration were conducted in triplicate. Mosquitoes that survived concentrations of 715 ng of plant extract were collected for RNA extraction and sequencing studies.

Synergistic assays using the CDC bottle bioassay

To determine synergism, a modification to the CDC bottle bioassay [34] was used. *Anopheles gambiae* (AKDR)

mosquitoes, which have demonstrated resistance to permethrin were used in these assays [35]. Non-blood fed adult female *An. gambiae* (AKDR), 3–5 days old ($n=25–30$), were topically exposed to ethanol or 1430 ng of plant extract while anaesthetized, as described above. The mosquitoes were transferred to a netted cup and observed for 1 h. After 1 h, actively flying mosquitoes were gently removed from the cups with a mouth aspirator and then transferred to bottles precoated with 21.5 µg of permethrin per bottle or acetone as a control treatment. Bottles were prepared 24 h prior to use [34]. The rate of knockdown/mortality was observed every 15 min for 120 min or until 100% mortality was achieved. Knockdown/mortality was recorded if mosquitoes were either inactive or the mosquitoes shed their legs or gave a sporadic jump without flight when the bottle was agitated/tapped. The experiment was conducted in duplicate. The experiment was repeated; results were pooled to give mortality rates.

RNA extraction and sequencing assays

RNA extraction assay

RNA extraction and sequencing studies were conducted on mosquitoes that survived the 24-h topical application of 715 ng of plant extract assays. Total RNA was isolated from pools containing ten mosquitoes each per plant assessed or from mosquitoes exposed to ethanol only. RNA was extracted using Arcturus®; PicoPure®; RNA isolation kit (Applied Biosystems, Vilnius, Lithuania). The extractions were conducted in triplicates. RNA was quantified using the Agilent RNA ScreenTape on the Agilent 4200 TapeStation (Agilent Technologies, CA, USA), according to the manufacturer's protocol.

Library construction and hybridization capture

RNA libraries were prepared for each pool of extracted RNA using TruSeq Stranded Total RNA kit (Illumina, CA, USA) using 14 cycles of PCR amplification. All protocols were performed following the manufacturer's instructions. Briefly, 500 ng of RNA per treatment was processed to deplete rRNA before being purified, fragmented, and primed with random hexamers. Fifty (50) ng of ribosomal-depleted primed RNA fragments were reverse transcribed into first strand cDNA using First-Strand Synthesis Actinomycin D mix and SuperScript II Reverse Transcriptase. RNA templates were removed, and a replacement strand was synthesized to generate ds cDNA. Libraries were purified using AMPure XP beads (Beckman Coulter, IN, USA). The quality and quantity were consistently evaluated on the Agilent 4200 TapeStation. The cDNA was stored at − 80 °C. The libraries were sequenced (2 × 125 bp, paired-end reads) on the Illumina HiSeq 2500 sequencer, using v2 chemistry. Sequencing was performed at the Biotechnology Core Facility at the CDC, Atlanta, GA, USA.

Read filtering and mapping

Sequenced reads were assigned to each sample and adaptors were removed. Overall read quality was checked for each sample using FastQC [36]. Reads were then filtered on the basis of their length, pairing, and quality using Trimmomatic version 0.39 [37]. Only paired reads were kept for mapping. Reads were mapped to the *An. gambiae* (PEST) and *An. funestus* (Fumoz) [38, 39] reference genomes obtained from VectorBase using hisat2 version 2.2.1 [40] with default parameters. SAMtools [41] and HTSeq version 0.13.5 [42] were used to sort the output files and count reads according to the respective genome annotation files obtained from VectorBase. The raw counts were processed using RStudio version 2021.09.0 [43], and the differential gene expression analysis was performed using the DESeq2 package [44]. Genes were considered differentially expressed if their absolute $\log_2$ fold change values were > 1 at FDR-adjusted $p<0.05$. The Panther classification system [45] was used for further characterization of gene enrichment of *An. gambiae* genes. For *An. funestus*, Panther classification was performed by determining the *An. gambiae* homologs for differentially expressed genes. XMgrace [46] was used to generate the volcano plot of differentially expressed CYP genes.

Table 1 Primers used in *An. gambiae* quantitative real-time PCR reactions

Gene ID *An. gambiae*	Name	Left primer	Right primer	References
AGAP008209	CYP6M1	GTGCTCGCCAAGCATAATGG	ACTTGCGTAGGGATTCTTTCA	[7]
AGAP008213	CYP6M3	ATCTGGAGCTGCTGAAGTGT	TTCATCTTCCCGGACGTGAA	
AGAP008214	CYP6M4	GGAACAGGAATCGAAGCGTC	GCACAGGAGTTTTGGAGCAA	
AGAP012291	CYP9J3	CACGTTTAACATGCGCCAAC	ATATCGCGCCACTTTTGTCC	
Housekeeping genes	GDPH	CTGCAAAAAGTCGATACCGC	CCTCGTACACGTACATCGTGA	
Housekeeping genes	RPS7gam	AGAACCAGCAGACCACCATC	GCTGCAAACTTCGGCTATTC	[7]

Validation of RNA sequencing from *An. gambiae* with qPCR

To confirm the expression of the genes observed in the RNA sequencing, CYP genes with low–high expression levels were selected. All primers (Table 1) were obtained from the Biotechnology Core Facility Branch (CDC). The primers were validated using conventional PCR. The PCR products were then visualized using the UVP GelStudio plus (Analytik Jena, CA, USA). Only primers that formed single-banded amplification products between 150 and 200 bp were used for the quantitative PCR assay. The qPCR amplification was carried out on a QuantStudio 6 Flex Real-Time PCR system (Applied Biosystems) using PowerUp SYBR Green Master Mix (Applied Biosystems). cDNA from each sample was used as a template in a three-step program as follows: Uracil-DNA glycosylase (UDG) activation at 50 °C for 2 min, DNA polymerase activation at 95 °C for 10 min, followed by 40 cycles of DNA denaturation for 15 s at 95 °C, DNA annealing and extension for 1 min at 60 °C, and a last DNA extension step of 15 s at 95 °C. The relative expression level and fold change (FC) of each target gene from treated samples relative to the untreated samples were calculated using the $2-\Delta\Delta CT$ method. Housekeeping genes were used to normalize the expression of the target genes.

Homology modelling

To ascertain binding affinity and possible interactions of the active metabolite within each extract with the CYP enzymes inhibited in vitro, as well as those found differentially expressed in the RNA-seq. studies, in silico models were generated. Preliminary structural models for CYPs 4G17, 6M2, 6P3, 9J3 (*An. gambiae*), and 6P9a (*An. funestus*), constructed using AlphaFold [47], were obtained from VectorBase [48]. Following structural alignment with *Homo sapiens* CYP3A4 (PDB ID: 6DAA) [49], the heme group coordinates were introduced for each CYP isoform.

Coordinates for the protein structures (CYPs 4G17, 6M2, 6P3, 6P9a, and 9J3) obtained as described above were subjected to a molecular dynamics simulation in water using GROMACS version 2020.4 [50], with the CHARMM27 force field [51]. To begin, each enzyme was centered in a cubic box 10 Å away from the edge with periodic boundary conditions. The box was subsequently solvated using spc water [52], prior to neutralizing each system with the appropriate number of counterions. The complete system was then subjected to 1000 steps of steepest descent energy minimization in preparation for the molecular dynamics simulation. Each simulation was initiated using the same equilibration scheme. Firstly, the initial velocities were randomly generated from a Maxwell–Boltzmann distribution at 300 K for a 100 ps equilibration under an NVT ensemble. The temperature coupling was controlled using a modified Berendsen thermostat [53] with a time constant of 0.1 ps. Secondly, the system was further equilibrated for 100 ps under an NPT ensemble. Pressure coupling was controlled using a Parrinello–Rahman barostat [54] with a time constant of 2.0 ps and an isothermal compressibility of 4.5×10^{-5} bar^{-1} in isotropic conditions.

The final system for each enzyme was used as the starting configuration for a 100-ns production run at 300 K, with structures saved every 100 ps. The LINCS algorithm [55] was used with an order of 4 to constrain bond lengths and water bond angles, allowing for an integration time step of 2 fs. Nonbonded interactions were calculated using a Verlet cutoff scheme [56], whereby interactions within 10 Å were calculated at every time step from a pair list that was updated every fifth time step. On the other hand, electrostatic interactions beyond 10 Å were approximated using the particle mesh Ewald summation [57]. Following the 100-ns simulation, the protein coordinates were extracted for molecular docking analysis.

Molecular docking

The protein structures for each enzyme (CYPs 4G17, 6M2, 6P3, 6P9a, and 9J3) were extracted from the final coordinates of the molecular dynamics simulations described above. Polar hydrogens were added using AutoDock tools [58], and the grid box was centered within each enzyme with dimensions in the *x*-, *y*-, and *z*-planes adequate to encompass its entire structure, thereby identifying the theoretical binding sites. Molecular structures for the compounds constituting the various treatments (piperine from *P. amalago* var. *amalago*; bryophyllin A, bryophyllin C, and luteolin-7-*O*-β-D-glucoside from *K. pinnata*; 2,3-diacetoxytormentic acid from *C. verticillata*) were generated using Avogadro version 1.90.0 [59], optimized, and suitably protonated at pH 7.4 before being prepared with AutoDock Tools [58]. Once both ligand and receptor files were ready, automated flexible docking was performed using AutoDock Vina [60], with no added restrictions. The best docking poses were selected in each case; the coordinates were visualized with VMD [61], through which images of the binding mode were generated. Lastly, LigPlot + version 2.2 [62], was applied to visualize the protein–ligand interactions, using default settings.

Data analysis

The inhibition concentrations at 50% enzyme activity (IC_{50}) were calculated in SigmaPlot v. 10. (Systat Software Inc.). The inhibitory concentrations are displayed as mean ± the standard error of the mean (SEM). The toxicity assays are presented as lethal doses at 50%

mortality ± 95% confidence interval (95% CI) per population. R (version 3.6.2) was used to calculate confidence intervals. Abbott's formula [63] (% Corrected Mortality = ((T−C)/(100−C)) × 100; where T is the total percent mortality in the treated group, and C is the percent mortality in the control group, providing that the control mortality was greater than 0% but less than or equal 20%) was used to correct the mortality rate in each treated group when necessary. The mortality in the control group for all toxicity assays was less than 20%. Statistical analyses were completed using SPSS for Windows (version 17.0). One-way analysis of variance (ANOVA) and *Post-hoc Tukey test* were used to determine significant differences ($p < 0.05$) between means where possible.

The differential gene expression analysis was performed using the DESeq2 package [44]. Genes were considered differentially expressed if their absolute $\log_2$ fold change values were > 1 at FDR-adjusted $p < 0.05$.

Table 3 Inhibition strength of Jamaican plant extracts that demonstrated strong inhibition of Anopheline CYPs

Plant extracts and compounds IC_{50}	CYP6P9a	CYP6P3	CYP6M2
Kalanchoe (Bryophyllum) pinnata µg/ml	> 20	> 20	3.52 ± 0.68
Condea (Hyptis) verticillata µg/ml	6.95 ± 0.11	> 20	> 20
Piper amalago var. *amalago* µg/ml	2.61 ± 0.17	5.84 ± 0.42	4.30 ± 0.42
Piperine µg/ml	8.01 ± 0.67	3.18 ± 0.17	0.14 ± 0.08
Deltamethrin µg/ml	1.34 ± 0.21	10.96 ± 3.57	8.91 ± 3.40
PBO µg/ml	0.15 ± 0.03	0.30 ± 0.02	0.06 ± 0.00

The Table shows the concentrations of *K. pinnata*, *C. verticillata*, *P. amalago amalago*, piperine—the active metabolite of *P. amalago amalago*, the insecticide deltamethrin and synergist piperonyl butoxide (PBO) that reduced CYP6P9a, CYP6P3, and CYP6M2-catalyzed diethoxyfluorescein activity by 50% (IC_{50}). Test compound concentrations varied between 0 and 200 µg/ml, as described in the Methods. Control enzyme activity (mean ± SEM) for CYP6P3, CYP6P9a, and CYP6M2 was 0.39 ± 0.01, 0.03 ± 0.05, and 0.02 ± 0.00 µM/min/pmol of CYP, respectively. Data are expressed as the mean concentration (mean ± SEM) to inhibit 50% enzyme activity for three independent experiments

Results

Effects of plant extracts on mosquito CYP in vitro

Single-point percentage inhibition was initially evaluated for eight water-based extracts of plants found in Jamaica, predominantly used for their medicinal and insecticidal activities. In vitro assays were conducted using resuspended lyophilized plant extracts to determine their ability to inhibit heterologously expressed anopheline CYP6P9a-, 6P3- and 6M2-mediated diethoxyfluorescein (DEF) activity. Inhibitory effects were compared using a standard extract concentration of 8.16 µg/ml, and > 60% inhibition of CYP activity was considered to be indicative of strong inhibition. The percentage inhibitory effects of the water-based extracts are presented in Table 2. *Piper amalago* var. *amalago* was the strongest inhibitor, producing > 70% inhibition of DEF activity against all three anopheline CYP enzymes, CYP6P9a, CYP6P3, and CYP6M2. *Condea verticillata* produced strong inhibition of CYP6P9a (65%) and moderate inhibition of CYP6M2 (41%) and CYP6P3 (31%), while *Kalanchoe pinnata* produced strong inhibition of CYP6M2 (73%) and weak inhibition of CYP6P9a (13%) and CYP6P3 (7%).

The inhibition strength (IC_{50}) of plant extracts *K. pinnata*, *C. verticillata*, and *P. amalago* var. *amalago* were further examined (Table 3) and compared to deltamethrin, a pyrethroid insecticide, and PBO, commonly used as a broad-spectrum inhibitor of mosquito CYPs activity [16, 64]. The extracts and compounds were categorized as potent ($IC_{50} < 1$ µg/ml), moderate (IC_{50} 1–10 µg/ml) and weak inhibitors ($IC_{50} > 10$ µg/ml) [22, 65] according to their activity as CYP inhibitors. PBO displayed potent activity against all three CYPs (IC_{50} values 0.06–0.30 µg/ml), while deltamethrin was a moderate inhibitor, with IC_{50} values in the range of 1.34–10.96 µg/ml. *K. pinnata* and *C. verticillata* extracts displayed moderate inhibition against single CYPs, CYP6M2 ($IC_{50} = 3.52$ µg/ml)

Table 2 Percentage inhibition of Anopheline CYP activity by Jamaican plant extracts at 8.16 µg/ml

Scientific name	Family	Voucher number	Local name	CYP6P9a	CYP6P3	CYP6M2
Bidens pilosa L.	Asteraceae	35366	Spanish Needle	10.43	10.92	11.74
Kalanchoe (*Bryophyllum*) *pinnata* (Lam.) Pers.	Crassulaceae	35466	Leaf of Life	12.52	7.34	73.00
Bursera simaruba (L.) Sarg.	Burseraceae	35363	Red Birch	7.93	0.63	a
Cinnamodendron corticosum Miers	Canellaceae	35375	Mountain Cinnamon	19.59	16.13	4.51
Croton linearis Jacq.	Euphorbiaceae	35365	Rock Rosemary	10.63	9.46	38.64
Guazuma ulmifolia Lam.	Malvaceae	35364	Bastard Cedar	24.59	11.84	22.86
Condea (Hyptis) verticillata Jacq.	Lamiaceae	35473	John Charles	65.01	31.07	41.08
Piper amalago var. *amalago*	Piperaceae	36616	Jointer	73.47	81.31	70.68

Data are expressed as the percentage mean of normal activity from three individual experiments. Control enzyme activity (mean ± SEM) for CYP6P9a, CYP6P3 and CYP6M2 was 0.08 ± 0.01, 0.31 ± 0.05, and 0.80 ± 0.03 abs/min/pmol of CYP, respectively

[a] Interference from the extract prevented fluorescence detection

and CYP6P9a (IC_{50} = 6.95 µg/ml), respectively, while *P. amalago* var. *amalago* extract displayed moderate inhibition, with IC_{50} values in the range of 2.61–5.84 µg/ml against all three enzymes.

Further GC–MS followed by HPLC analysis (Supplemental 2) of *P. amalago* var. *amalago* extract revealed piperine to be the most abundant compound. The inhibitory property of piperine was assessed. The inhibitory properties of piperine were similar to that of *P. amalago* var. *amalago*. However, piperine potently inhibited CYP6M2 (IC_{50} = 0.14 µg/ml), with values comparable to PBO, and moderately inhibited CYP6P3 (IC_{50} = 3.18 µg/ml), and CYP6P9a (IC_{50} = 8.01 µg/ml).

Effects of plant ethanol extracts on Mosquito in vivo

To determine whether the moderate inhibition of mosquito CYPs by the plant extract observed in vitro was indicative of their potential as insecticides and/or insecticide synergists against the mosquitoes with the respective CYPs, the insecticidal activities of prepared extracts from *K. pinnata*, *P. amalago* var. *amalago*, and *C. verticillata* against *Anopheles* mosquitoes was evaluated. An ethanol extract of each plant was prepared to facilitate topical application of the extracts and to elute similar chemical composition to that of the water-based plant extracts. The 50% lethal dose (LD_{50}) values were similar for *K. pinnata* (282.37 ± 17.94 ng/mosquito) and *P. amalago* var. *amalago* (368.42 ± 70.50 ng/mosquito) (Fig. 1). *C. verticillata*, however, failed to produce mortality > 30% at the highest concentration used for either *An. gambiae* (G3) or *An. funestus* (Fumoz) after 24 h of exposure, as such, LD_{50}s for *C. verticillata* could not be generated.

Of the three plant extracts assessed for their insecticidal activities, *K. pinnata* was the most toxic towards *An. gambiae.* The synergistic activity of the ethanol

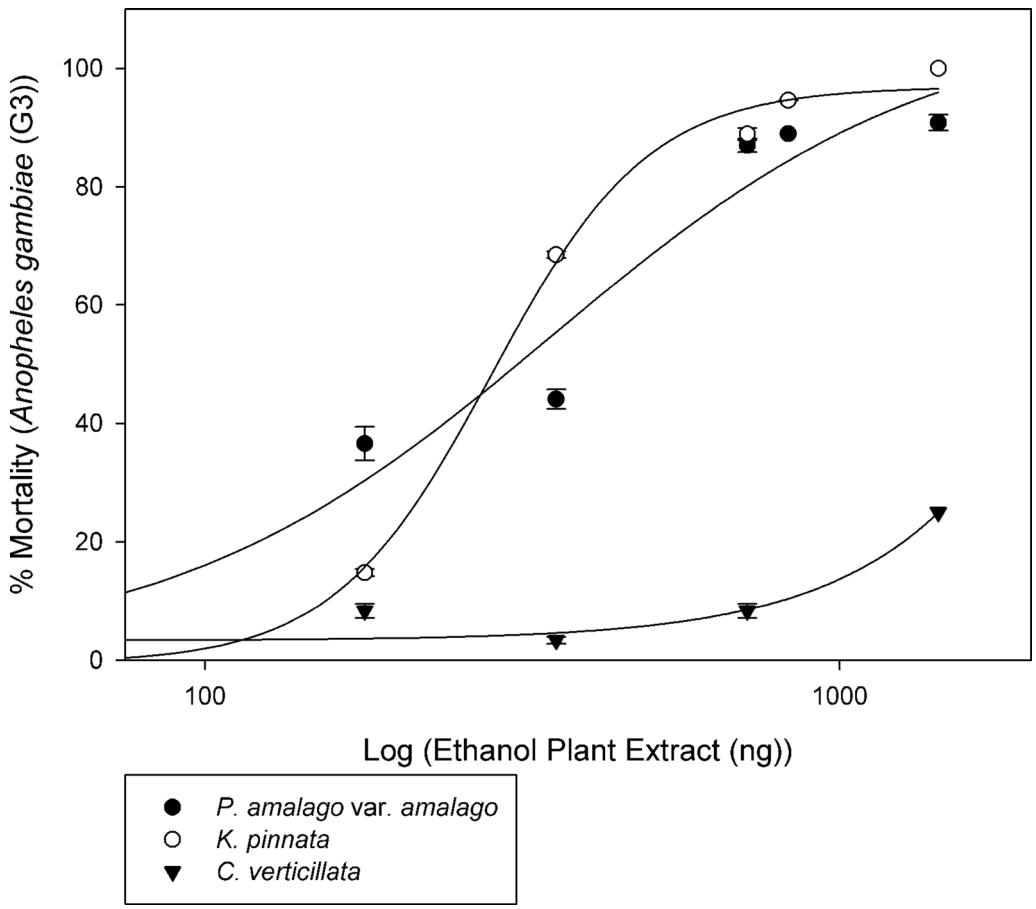

Fig. 1 Mortality studies on *An. gambiae* with *Piper amalago* var. *amalago, Kalanchoe pinnata* or *Condea verticillata*. Non-blood-fed female (3–5 days old) *An. gambiae* were topically treated with plant extract for 24 h. *P. amalago* var. *amalago, K. pinnata* or *C. verticillata* was applied to *An. gambiae.* The lethal dose that resulted in 50% mortality (LD_{50}) was 368.42 and 282.37 ng/mosquito for *P. amalago* var. *amalago* and *K. pinnata,* respectively. The extract of *C. verticillata* resulted in low toxicity towards *An. gambiae*, causing 25% mortality at 1430 ng/mosquito. The data points are expressed as mean ± 95% confidence intervals; n = 20–25 mosquitoes per replicate; average weight of mosquitoes = 0.4 mg

extract from *K. pinnata* was tested with permethrin against *An. gambiae* (AKDR), a permethrin-resistant strain. The highest prepared dose (1.43 µg/mosquito) of *K. pinnata* ethanol extract was initially applied to the mosquitoes. After 1 h, the mosquitoes were gently placed in 250-ml Wheaton bottles precoated with 21.5 µg of permethrin. Synergy with *K. pinnata* produced rapid knockdown/mortality, with 83.19% death occurring within 30 min, followed by a gradual decline and 100% mortality after 75 min. By contrast, permethrin alone produced a delayed response, with 90% dead after 75 min and 100% mortality by 90 min (Fig. 2).

RNA sequencing for CYP genes

RNA sequencing of mosquitoes treated with the plant extracts was conducted to determine whether the extracts could modulate CYP gene activity in vivo. A concentration that produced greater than 50% mortality was selected to observe changes in gene regulation within a 24-h period. Topical treatment of female *An. gambiae* with 715 ng of *P. amalago* var. *amalago* resulted in the upregulation of 229 genes and the downregulation of 479 genes ($|\log_2$ fold change$|>1$; FDR-adjusted $p<0.05$) compared to the untreated control. Similarly, topical application of 715 ng of *K. pinnata* induced the upregulation of 313 genes and downregulation of 580 genes ($|\log_2$ fold change$|>1$; FDR-adjusted $p<0.05$) compared to the untreated control (Table 4).

In both treatments, commonly upregulated genes included glutathione *S*-transferases, lactate dehydrogenases, heme peroxidases, and α-tubulin, while commonly downregulated genes included trypsins, C-type lectins, lipases, chitinases, and cuticular proteins. CYPs 6M1, 6M3, 6M4, and 9J3 were upregulated following both treatments, while CYP 4G17 was downregulated following both treatments (Fig. 3). Interestingly CYPs 6M2 and 6Z2 were significantly upregulated by *P. amalago* var. *amalago*, whereas *K. pinnata* had little to no effect on the expression of these enzymes.

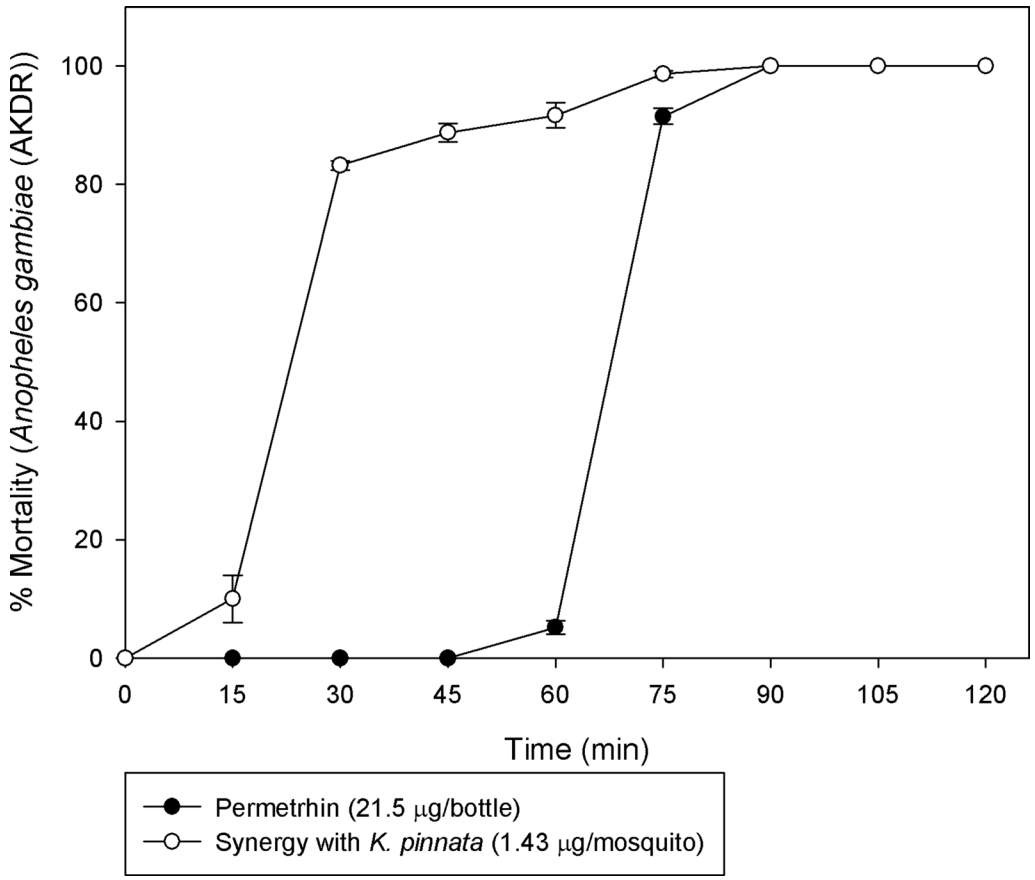

Fig. 2 Synergistic studies with Permethrin and *Kalanchoe pinnata* extract. Non-blood-fed female (3–5 days old) female *An. gambiae* (AKDR) were topically treated with 1.43 µg of the *K. pinnata* plant extract and observed for 1 h. After 1 h, the mosquitoes were gently transferred to bottles pretreated with 21.5 µg of permethrin. Mosquitoes were observed until 100% knockdown/mortality (the data points are expressed as mean ± confidence intervals (CI); n = 71–88 mosquitoes; average weight of mosquitoes: 0.35 mg)

Table 4 Differential gene expression in *An. gambiae* treated with *Piper amalago* var. *amalago* or *Kalanchoe pinnata* compared to the untreated control

Top 50 differentially expressed genes that were upregulated ($|\log_2$ fold change$|>1$; FDR-adjusted $p<0.05$) by at least one treatment, classified according to Panther

Gene ID	Gene name	Product description	$\log_2$ fold change	
			***P. amalago* vs. ethanol only treated**	***K. pinnata* vs. ethanol only treated**
RNA metabolism				
AGAP029470	–	SAM domain-containing protein	2.01	2.24
Cytoskeleton				
AGAP007122	–	Tubulin, alpha 1	1.97	2.11
AGAP003352	–	Stomatin (EPB72)-like 3	1.71	1.85
Metabolite interconversion				
AGAP004383	*GSTD10*	Glutathione *S*-transferase delta class 10	4.76	5.09
AGAP013327	*HPX15*	Heme peroxidase 15	3.02	3.20
AGAP008212	*CYP6M2*	Cytochrome P450	2.89	0.10
AGAP008209	*CYP6M1*	Cytochrome P450	2.44	2.74
AGAP004880	–	L-Lactate dehydrogenase	3.41	3.54
AGAP011806	–	NADH dehydrogenase 1 beta subcomplex 4	1.39	2.61
AGAP008213	*CYP6M3*	Cytochrome P450	2.33	1.67
AGAP007300	–	Unspecified product	1.90	2.15
AGAP008218	*CYP6Z2*	Cytochrome P450	1.98	0.15
AGAP012388	–	DUF1298 domain-containing protein	1.86	1.97
AGAP008214	*CYP6M4*	Cytochrome P450	1.62	1.98
AGAP012296	*CYP9J5*	Cytochrome P450	1.92	0.90
Protein modification				
AGAP005125	–	Tripartite motif-containing protein 71	1.77	1.87
Transfer/Carrier				
AGAP000427	–	Vitellogenin receptor	2.45	2.36
Translation				
AGAP007858	–	Lysyl-tRNA synthetase, class II	1.89	2.20
Transport				
AGAP005795	–	Sodium-coupled monocarboxylate transporter 1	2.52	2.87
AGAP008437	*ABCC9*	ATP-binding cassette transporter family C member 9	2.30	1.41
AGAP008436	*ABCC11*	ATP-binding cassette transporter family C member 11	1.86	1.95
AGAP008738	–	Unspecified product	1.67	1.94
Unclassified				
AGAP028182	–	Ankyrin repeat domain-containing protein	2.90	2.50
AGAP005987	–	Unspecified product	2.77	2.83
AGAP007959	–	Unspecified product	2.54	2.76
AGAP006385	–	Unspecified product	1.46	2.71
AGAP007650	–	Growth arrest and DNA-damage-inducible protein	1.99	2.68
AGAP003488	–	Nucleotide exchange factor SIL1	1.71	2.63
AGAP001610	–	Unspecified product	1.80	2.50
AGAP006367	–	Unspecified product	2.39	2.30
AGAP003757	–	Unspecified product	1.84	2.28
AGAP010658	–	Unspecified product	1.58	2.27
AGAP007823	–	Unspecified product	1.96	2.22
AGAP028652	–	Unspecified product	1.86	2.18
AGAP012443	–	Unspecified product	1.54	2.17
AGAP028566	–	Unspecified product	2.12	1.99

Table 4 (continued)

Top 50 differentially expressed genes that were upregulated (|log_2 fold change|> 1; FDR-adjusted p < 0.05) by at least one treatment, classified according to Panther

Gene ID	Gene name	Product description	Log_2 fold change	
			***P. amalago* vs. ethanol only treated**	***K. pinnata* vs. ethanol only treated**
AGAP013745	–	HTH OST-type domain-containing protein	1.93	2.09
AGAP009682	–	Unspecified product	1.72	1.95
AGAP028655	–	Unspecified product	1.73	2.12
AGAP028201	–	Unspecified product	1.99	2.08
AGAP029097	–	Unspecified product	1.75	2.06
AGAP005253	–	Unspecified product	1.76	2.03
AGAP013506	*UPD3A*	JAK/STAT pathway cytokine unpaired 3 variant A	1.69	1.98
AGAP028541	–	Unspecified product	1.95	1.77
AGAP011981	–	Unspecified product	1.72	1.94
AGAP009404	–	*N*-Acetyllactosaminide beta-1,3-*N*-acetylglucosaminyltransferase	1.94	1.52
AGAP009656	–	C2H2-type domain-containing protein	1.94	1.52
AGAP029285	–	Unspecified product	1.42	1.88
AGAP029766	–	Polypeptide *N*-acetylgalactosaminyltransferase	1.50	1.84
AGAP006222	–	Glucosyl/glucuronosyl transferase	1.84	0.00

Top 50 differentially expressed genes that were downregulated (|log_2 fold change|> 1; FDR-adjusted p < 0.05) by at least one treatment, classified according to Panther

Gene ID	Gene name	Product description	Log_2 fold change	
			***P. amalago* vs. ethanol only treated**	***K. pinnata* vs. ethanol only treated**
Binding				
AGAP001969	–	Polyubiquitin	−4.59	−5.09
AGAP029559	*CTLMA6*	C-type lectin (mannose binding)	−4.27	−4.25
Catalytic activity				
AGAP001748	–	Chitin synthase	−4.11	−4.28
AGAP008295	*TRYP2*	Trypsin 2	−3.62	−2.77
AGAP008290	*TRYP6*	Trypsin 6	−3.31	−2.49
AGAP008293	*TRYP7*	Trypsin 7	−2.87	−3.19
AGAP001594	–	Unspecified product	−2.87	−3.18
AGAP008487	–	Sphingomyelin phosphodiesterase	−3.14	−3.00
Structural molecule activity				
AGAP000047	*CPR130*	Cuticular protein RR-2 family 130	−8.08	−8.06
AGAP000820	*CPR125*	Cuticular protein RR-2 family 125	−5.85	−6.54
AGAP000344	*CPR127*	Cuticular protein RR-1 family 127	−4.93	−4.91
AGAP009871	*CPR75*	Cuticular protein RR-1 family 75	−3.40	−4.32
AGAP005456	*CPR15*	Cuticular protein RR-1 family 15	−3.91	−3.73
AGAP006001	*CPR26*	Cuticular protein RR-1 family 26	−2.89	−3.66
AGAP009874	*CPR76*	Cuticular protein RR-1 family 76	−2.95	−3.49
Unclassified				
AGAP008449	*CPLCG5*	Cuticular protein CPLCG family (CPLCG5)	−9.09	−10.34
AGAP006147	–	Unspecified product	−9.52	−9.60
AGAP008447	*CPLCG4*	Cuticular protein CPLCG family (CPLCG4)	−8.38	−9.20
AGAP006148	*CPLCA3*	Cuticular protein 3 in CPLCA family	−6.56	−9.41
AGAP009759	*CPLCP12*	Cuticular protein CPLCP12	−8.01	−7.70

Table 4 (continued)

Top 50 differentially expressed genes that were downregulated (|$\log_2$ fold change|> 1; FDR-adjusted p < 0.05) by at least one treatment, classified according to Panther

Gene ID	Gene name	Product description	$\log_2$ fold change	
			***P. amalago* vs. ethanol only treated**	***K. pinnata* vs. ethanol only treated**
AGAP007980	*CPCFC1*	Cuticular protein CPCFC family (CPCFC1)	−7.31	−7.59
AGAP006829	*CPR59*	Cuticular protein RR-1 family 59	−6.85	−7.38
AGAP008450	–	Unspecified product	−6.37	−7.17
AGAP006149	*CPLCX3*	Cuticular protein unclassified	−5.39	−6.92
AGAP009758	*CPLCP11*	Cuticular protein CPLCP11	−6.39	−5.92
AGAP028680	–	F-box domain-containing protein	−4.95	−6.31
AGAP028679	–	Unspecified product	−4.84	−6.20
AGAP004135	–	Yellow-e	−5.98	−5.76
AGAP029797	–	Unspecified product	−4.51	−5.66
AGAP003308	*CPAP3-C*	Cuticular protein	−4.78	−4.70
AGAP004690	*CPF3*	Cuticular protein 3 from fifty-one aa family	−1.92	−4.21
AGAP003582	–	D-Xylulose reductase A	−3.00	−3.95
AGAP000745	–	Alanine transaminase	−3.35	−3.91
AGAP006434	–	Unspecified product	−3.60	−3.90
AGAP011530	–	Collagen, type I/II/III/V/XI/XXIV/XXVII alpha	−3.43	−3.89
AGAP008782	–	23.4 kDa salivary protein	−3.76	−3.58
AGAP006146	*CPLCA2*	Cuticular protein 2 in CPLCA family	−3.12	−3.74
AGAP006480	–	Unspecified product	−3.24	−3.72
AGAP007416	–	MH2 domain-containing protein	−3.08	−3.58
AGAP003334	*CPLCX2*	Cuticular protein unclassified	−3.54	−3.52
AGAP008281	*D7r4*	D7 short form salivary protein	−2.60	−3.47
AGAP003261	–	ZP domain-containing protein	−3.43	−3.48
AGAP000696	–	Cuticular protein RR-2 family 125	−3.26	−3.31
AGAP011930	–	Unspecified product	−2.67	−3.29
AGAP000988	*CPAP3-A1c*	F-type H^+-transporting ATPase subunit b	−3.25	−3.12
AGAP011937	–	Unspecified product	−3.24	−3.14
AGAP006964	–	Pyroglutamyl-peptidase	−2.68	−3.21
AGAP006433	–	Unspecified product	−2.91	−3.16
AGAP008512	–	NodB homology domain-containing protein	−2.82	−3.16
AGAP028135	–	Lipase domain-containing protein	−3.07	−3.15

According to Gene Ontology analysis, both treatments influenced heterocyclic and organic cyclic compound binding and oxidoreductase activity under the molecular function category, cellular anatomical entity and intracellular anatomical structure under the cellular component category, and cellular process and macromolecule metabolic process under the biological process category. Panther classification revealed that proteins within the transport, metabolite interconversion, and protein modification classes were widely upregulated and downregulated following both treatments.

Quantitative RT–PCR was used to validate the directional fold change (FC) of four CYP gene isoforms (6M1, 6M3, 6M4 and 9J3), relative to two housekeeping genes, $GDPH_{gam}$ and $S7_{gam}$ (Fig. 4). The Pearson correlation coefficients, $r = 0.927$, demonstrated similar gene expression levels between the assays. The qRT–PCR analysis supports the directionality of changes in expression levels as estimated by RNA sequencing.

Following topical treatment of *An. funestus* (Fumoz) with 715 ng of *C. verticillata*, 102 genes were upregulated and 14 genes were downregulated (|$\log_2$ fold change|> 1; FDR-adjusted $p < 0.05$) compared to the ethanol only

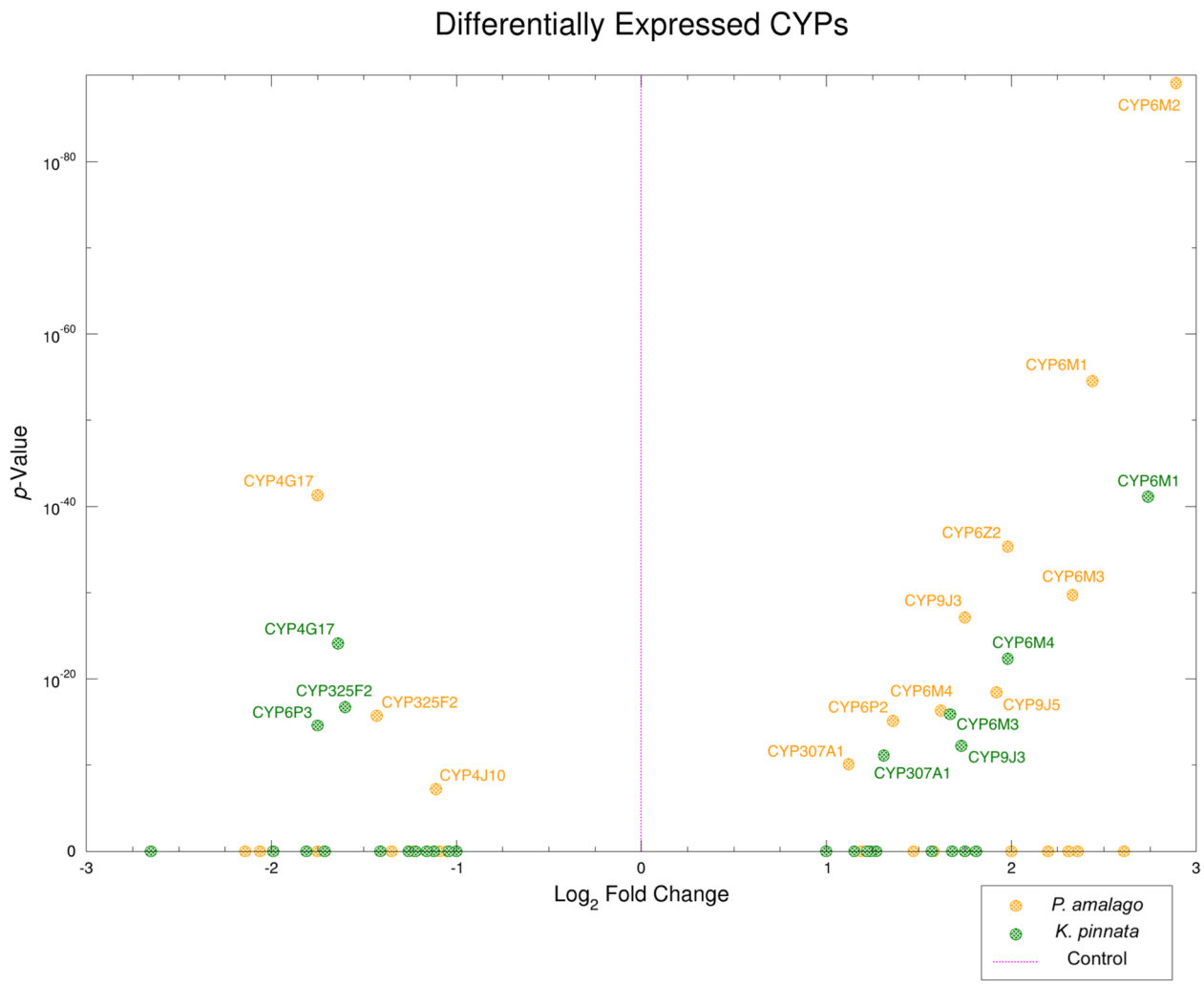

Fig. 3 RNA sequencing of CYP gene expression in *An. gambiae* treated with *Piper amalago* var. *amalago* or *Kalanchoe pinnata*. CYP genes that were differentially expressed with respect to the control ($|\log_2$ fold change$| > 1$; FDR-adjusted $p < 0.05$) following topical application of either *P. amalago var. amalago* or *K. pinnata* (715 ng of plant extract) to *An. gambiae* (n = 10 mosquitoes per treatment per replicate)

treatment (Table 5). The majority of upregulated genes were eukaryotic small unit ribosomal RNAs (unable to be classified by Panther). Genes classified as related to binding were significantly downregulated (e.g., homeobox domain-containing protein), whereas genes classified as related to catalytic activity (e.g., peptidase S1 domain-containing protein) and binding (e.g., G patch domain-containing protein) were upregulated.

It should also be mentioned that several genes were highly differentially expressed ($|\log_2$ fold change$| > 2$), for which a *p*-value could not be calculated. While they are not included in the table, some notable genes deserve mention. Among those downregulated were TIL domain-containing protein and dynein heavy chain. Among those upregulated were chitinase and aromatic L-amino-acid decarboxylase. This category of differentially expressed genes also constituted CYPs 325F1, 4H18, and 9J4 among those upregulated, whereas CYP 6AD1 was downregulated.

According to Gene Ontology analysis, treatment with *C. verticillata* influenced binding, catalytic activity, and transmembrane transporter activity under the molecular function category, cellular anatomical entity and retromer complex under the cellular component category, and cellular process, metabolic process, and localization under the biological process category.

Modelling

In silico modelling was used to investigate compound interactions in the CYP active sites and to estimate

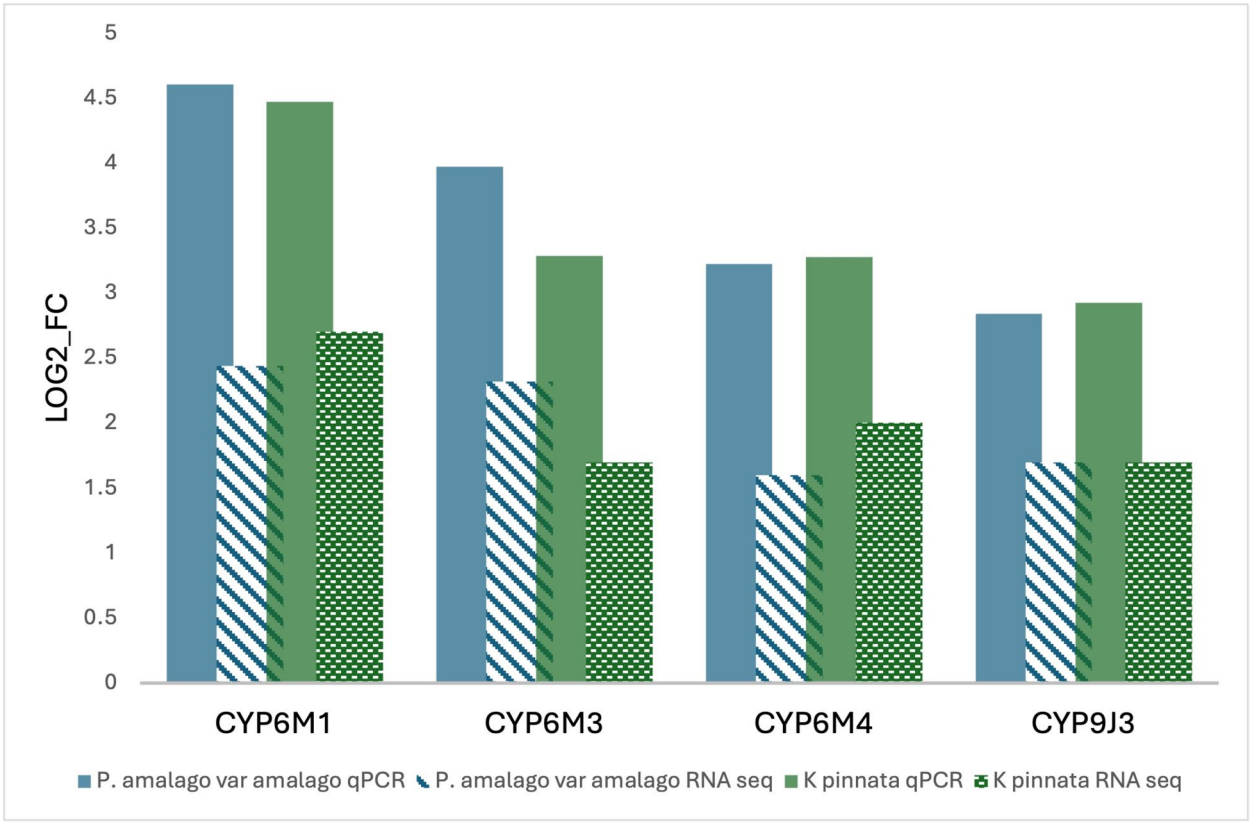

Fig. 4 Gene expression correlation between RNA sequencing and qPCR from *An. gambiae* treated with *Piper amalago* var. *amalago* or *Kalanchoe pinnata*. RNA sequencing validation by qPCR was conducted on mosquitoes previously treated with 715 ng of extract to corroborate the direction of fold change observed with RNA sequencing. RNA was extracted after 24-h exposure (n = 10 mosquitoes per treatment per replicate)

docking strengths. Following on the information garnered from the RNA sequencing results, in silico modelling was conducted on CYPs that were differentially expressed in mosquitoes treated with *P. amalago* var. *amalago, K. pinnata* or *C. verticillata* ethanol extracts, as well as CYP enzymes used in the in vitro assays. The compounds modelled were as follows: piperine, confirmed in this study by GC–MS and HPLC analysis from *P. amalago* var. *amalago* extract (supplemental 2); 2,3-diacetoxytormentic acid, confirmed in the *C. verticillata* ethanolic extract [22]; bryophyllin A, bryophyllin C, and luteolin-7-*O*-β-D-glucoside, reported to account for the insecticidal activity of *K. pinnata* [20]. When evaluating the potential of compounds in drug discovery, a docking threshold of − 29 kJ·mol^{-1} can be considered as a starting point to identify candidates with good binding [66], whereby more negative values indicate stronger binding. As a reference point, the values in the binding Mother of All Databases (MOAD) are normally distributed around approximately − 37 kJ·mol^{-1} [67]. A dissociation constant (K_d) of 1–100 nM, suggestive of excellent inhibition, roughly translates to a binding affinity of − 40 to − 50 kJ·mol^{-1} [68].

Kalanchoe pinnata extract

Bryophillins A and C and luteolin-7-*O*-β-D-glucoside were docked into the CYPs 4G17, 6M2, 6P3, and 9J3 from *An. gambiae*. Bryophillin A presented binding affinities ranging from − 39.3 (CYP9J3) to − 47.7 kJ·mol^{-1} (CYP6P3), while Bryophillin C presented binding affinities ranging from − 31.8 (CYP4G17) to − 49.4 kJ·mol^{-1} (CYP6P3). Luteolin-7-*O*-β-D-glucoside presented its highest binding affinity (− 46.0 kJ·mol^{-1}) in CYP6M2 and lowest binding affinity (− 36.4 kJ·mol^{-1}) in CYP4G17 (Table 6). All three compounds exhibited π–π stacking interactions with conserved phenylalanine residues in the respective active sites, along with occasional hydrogen bonds (Fig. 5). The strongest binding was observed

Table 5 Differential gene expression in *An. funestus* treated with *C. verticillata* compared to the untreated control

Top 50 differentially expressed genes that were upregulated by treatment *C. verticillata* ($\|\log_2$ fold change$\| > 1$; FDR-adjusted $p < 0.05$), classified according to Panther			
Gene ID	**Gene symbol**	**Product description**	**$\log_2$ fold change**
			***C. verticillata* vs. ethanol only treated**
Binding			
AFUN006552	–	G-patch domain-containing protein	3.74
AFUN007199	–	Polyadenylate-binding protein	3.46
AFUN021449	–	Troponin C	1.86
AFUN005374	–	Phosphoserine phosphatase	1.68
AFUN009447	*RpS25*	40S ribosomal protein S25	1.34
Catalytic activity			
AFUN022310	–	Peptidase S1 domain-containing protein	2.85
AFUN004890	–	Acyl-CoA dehydrogenase	1.98
AFUN008039	–	Nucleoside diphosphate kinase	1.86
AFUN006334	–	Choline/ethanolamine kinase	1.74
AFUN004178	–	Phosphoenolpyruvate carboxykinase (GTP)	1.56
AFUN021716	–	4-Hydroxyphenylpyruvate dioxygenase	1.52
Translation			
AFUN007816		Eukaryotic translation initiation factor 6	2.17
Structural Molecule Activity			
AFUN021595		Cuticular protein RR-1 family	1.55
Unclassified			
AFUN018774	–	Unspecified product	4.90
AFUN010671	–	CLIP-domain serine protease	3.03
AFUN016466	*SRPN11*	Serine protease inhibitor (serpin) 11	2.99
AFUN019721	–	Chitin-binding type-2 domain-containing protein	2.62
AFUN006360	–	Unspecified product	2.33
AFUN009998	–	Unspecified product	2.30
AFUN004722	–	Unspecified product	2.17
AFUN000713	–	Protein flightin	2.08
AFUN010326	–	Unspecified product	2.04
AFUN007648	–	Cubilin	1.93
AFUN004703	–	Unspecified product	1.91
AFUN007491	–	Unspecified product	1.79
AFUN022138	–	Poly(U)-specific endoribonuclease	1.71
AFUN019741	–	Unspecified product	1.71
AFUN007811	–	30 kDa salivary antigen family protein	1.71
AFUN005860	–	CLIP-domain serine protease	1.67
AFUN011122	–	Unspecified product	1.63
AFUN003703	–	Unspecified product	1.62
AFUN016374	*NimB2*	Nimrod B2	1.61
AFUN008531	–	Unspecified product	1.60
AFUN006361	–	Unspecified product	1.57
AFUN006915	*DEF1*	Defensin anti-microbial peptide	1.57
AFUN008739	–	Unspecified product	1.56
AFUN004736	–	Unspecified product	1.55
AFUN016569	–	Unspecified product	1.54
AFUN008289	–	Unspecified product	1.51
AFUN022193	–	Unspecified product	1.51

Table 5 (continued)

Top 50 differentially expressed genes that were upregulated by treatment *C. verticillata* ($|\log_2$ fold change$| > 1$; FDR-adjusted $p < 0.05$), classified according to Panther

Gene ID	Gene symbol	Product description	$\log_2$ fold change *C. verticillata* vs. ethanol only treated
AFUN021309	–	Unspecified product	1.51
AFUN021780	–	Unspecified product	1.49
AFUN003274	*LRIM19*	Leucine-rich immune protein (Coil-less)	1.45
AFUN005947	–	Unspecified product	1.45
AFUN020976	–	Unspecified product	1.42
AFUN018799	–	PMSR domain-containing protein	1.41
AFUN018668	–	PMSR domain-containing protein	1.39
AFUN016413	–	Unspecified product	1.38
AFUN022012	–	Unspecified product	1.36
AFUN009926	–	Unspecified product	1.34

Top 50 differentially expressed genes that were downregulated ($|\log_2$ fold change$| > 1$; FDR-adjusted $p < 0.05$) by treatment *C. verticillata*, classified according to Panther

Gene ID	Gene symbol	Product description	$\log_2$ fold change *C. verticillata* vs. ethanol only treated
Binding			
AFUN004151	–	Homeobox domain-containing protein	−1.30
AFUN010213	*RpL36*	60S ribosomal protein L36	−1.17
AFUN022227	–	Niemann-Pick Type C-2	−1.16
AFUN003198	*RpS26*	40S ribosomal protein S26	−1.03
No classification			
AFUN018847	–	Thioester-containing protein	−2.86
AFUN018885	–	Unspecified product	−2.16
AFUN004001	–	Unspecified product	−1.32
AFUN006496	–	Unspecified product	−1.21
AFUN006704	–	5′ nucleotidase, ecto	−1.13
AFUN004873	–	Unspecified product	−1.13
AFUN001787	–	Unspecified product	−1.13
AFUN008722	–	Unspecified product	−1.09
AFUN018908		Solute carrier family 15 member	−1.06
AFUN016019	–	Unspecified product	−1.03

Table 6 Binding affinities (in kJ/mol) of the identified compounds toward the selected CYP enzymes according to molecular docking studies

Plant	Compound/Enzyme	CYP4G17	CYP6M2	CYP6P3	CYP6P9a	CYP9J3
P. amalago var. *amalago*	Piperine	−39.7	−35.6	−38.5	−36.4	−31.0
C. verticillata	2,3-Diacetoxytormentic acid				−44.4	
K. pinnata	Bryophyllin A	−42.3	−44.4	−47.7		−39.3
K. pinnata	Bryophyllin C	−31.8	−46.9	−49.4		−39.3
K. pinnata	Luteolin-7-O-β-D-glucoside	−36.4	−46.0	−43.9		−37.2

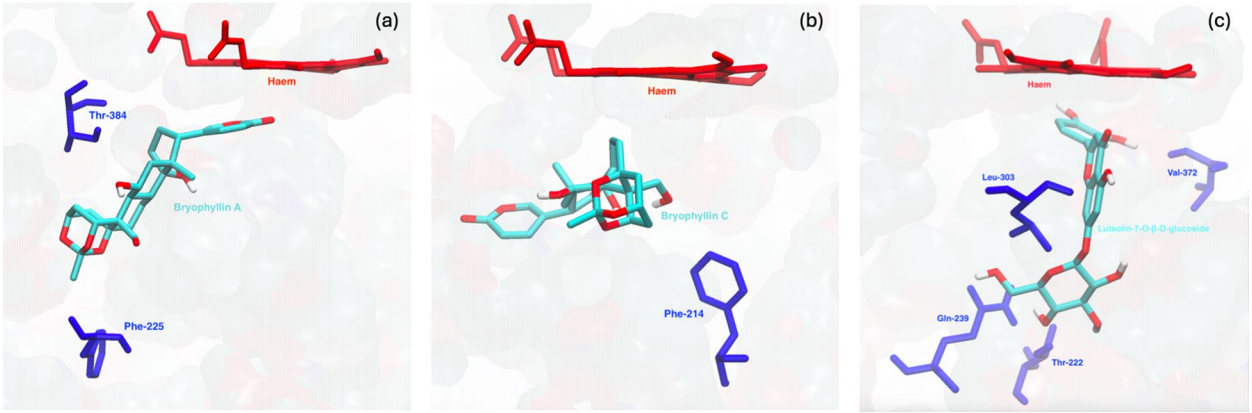

Fig. 5 Best theoretical binding poses achieved for *K. pinnata* compounds. Bryophyllin A (**a**), bryophyllin C (**b**) and luteolin 7-O-β-D-glucoside (**c**) complexed with CYPs 6P3, 6P3 and 6M2, respectively. CYPs are shown in surface representation (grey), with key residues identified for binding shown (blue) and the heme group (red) shown in stick representation. The ligands are also shown in stick representation, colored according to atom type (C—cyan; N—blue; O—red; H—white)

for CYPs 6M2 and 6P3, suggesting that treatment with *K. pinnata* may provide efficient inhibition or occupation of the CYPs 6P3 and 6M2 active sites, bypassing a major mechanism of insecticide resistance in mosquitoes [5, 6]. This would accordingly improve insecticidal activity when applied in conjunction with commonly used insecticides, as observed in the synergist application (Fig. 2) with permethrin on *An. gambiae* (AKDR).

Condea verticillata extract

2,3-Diacetoxytormentic acid was docked into CYP6P9a from *An. funestus*, presenting an excellent binding affinity of − 44.4 kJ·mol^{-1} (Table 6). Its binding pose was predominantly mediated by π−π stacking interactions with conserved phenylalanine residues in the active site (Fig. 6). This may underlie the potential for the mosquito-specific insecticidal activity of *C. verticillata* extracts, as also demonstrated in the inhibitory assay (Table 3). 2,3-Diacetoxytormentic acid was previously found to have insecticidal activity, albeit at low levels [19, 22].

Piper amalago var. *amalago* extract

Piperine was docked into all CYPs evaluated (4G17, 6M2, 6P3, and 9J3 from *An. gambiae* and 6P9a from *An. funestus*). Good binding affinity (exceeding − 35 kJ·mol^{-1}) was observed in all cases but CYP9J3 (− 31.0 kJ·mol^{-1}) (Table 6). A common feature was once again π−π stacking interactions with conserved phenylalanine residues in the active site, along with hydrogen bonding in some cases (Fig. 7). This relatively broad activity of piperine, a compound common to Piperaceae family [69–71], may be due to its methylenedioxyphenyl group, which is well established to have CYP-inhibitory properties via forming intermediates with the heme group [72]. In the four cases with strong affinity, the best binding mode presented this functional group toward the iron center of the heme, speaking to the possibility of this interaction, as well as suggesting the potential nonspecificity of piperine's inhibitory activity observed (Table 3). This compound was also found to have synergistic activity when combined with insecticides [29], in line with its demonstrated synergistic [73], *cyp* induction [74], inhibition of heterologously expressed mosquito larvae CYPs [75], insecticidal [76, 77], growth-regulating [78], anti-foraging [29], and repellency [79] properties. The inhibitory assays (Table 3) also revealed the broad-spectrum activity of piperine.

Discussion

The secondary metabolites of plants provide diverse chemical structures with multiple biological activities. The study identified compounds that might be used as synergists to inhibit CYPs associated with the detoxification of insecticides in mosquitoes. Extracts were prepared from plants for their potential to inhibit the activities of representative CYPs commonly overexpressed in African malaria vectors associated with pyrethroid resistance, *An. gambiae* CYP6P3 and CYP6M2 and *An. funestus* CYP6P9a, and their activity in vivo confirmed.

Of the eight aqueous plant extracts explored, *P. amalago* var. *amalago, C. verticillata*, and *K. pinnata* demonstrated specificity for one or more recombinant CYPs, overexpressed in *Anopheles* mosquitoes resistant to pyrethroids, with IC_{50}s < 10 µg/ml in vitro (Table 3). These values were comparable to the inhibitory properties of the insecticidal compound deltamethrin and the synergist PBO, suggesting that the compounds have

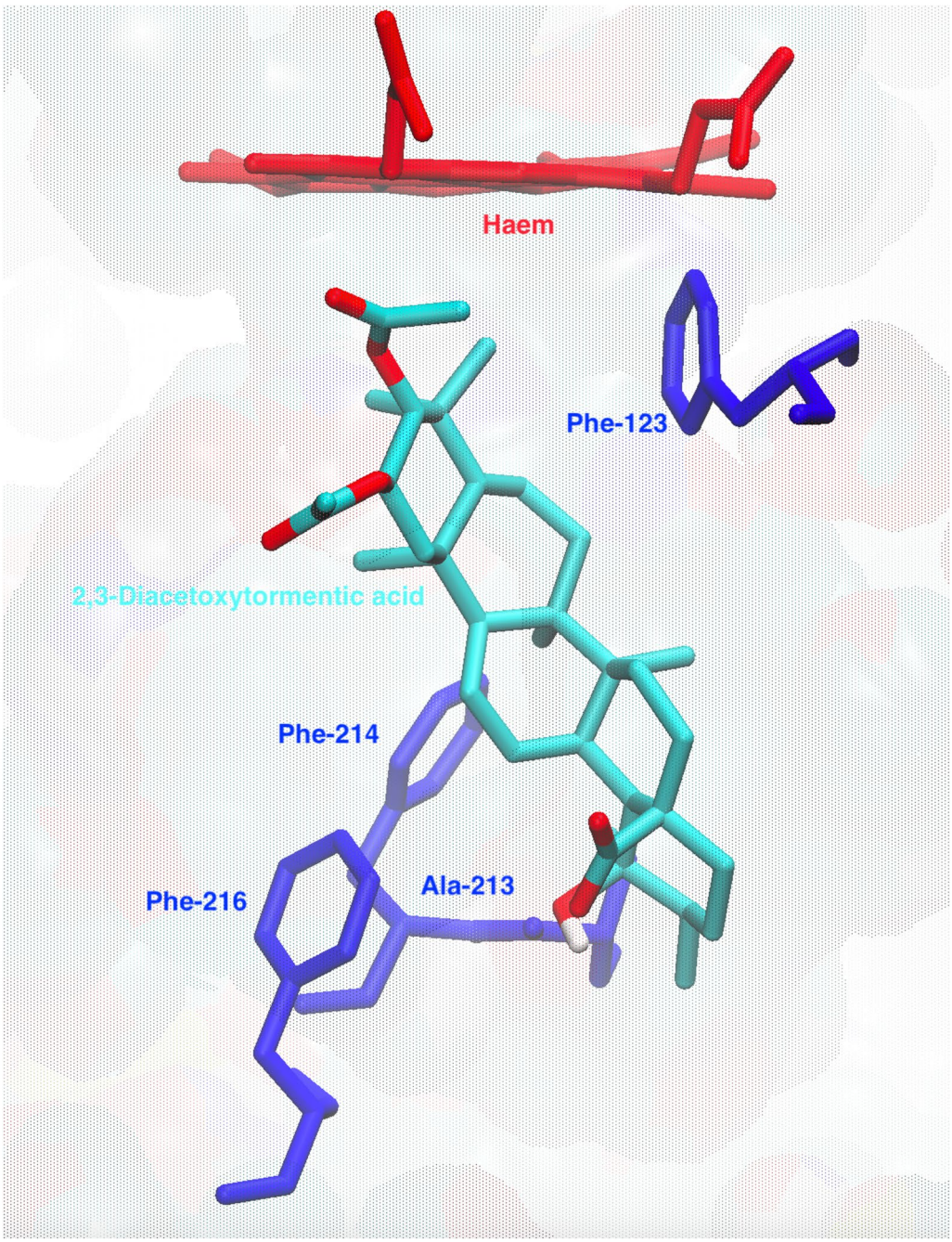

Fig. 6 Best theoretical binding pose achieved for *C. verticillata* compound. 2,3-Diacetoxytormentic acid complexed with CYP6P9a. CYP 6P9a is shown in surface representation (grey), with key residues identified for binding shown (blue) and the heme group (red) shown in stick representation. The ligand is also shown in stick representation, colored according to atom type (C—cyan; N—blue; O—red; H—white)

potential as insecticide synergists. As such, these three plant extracts were assessed for their effect in vivo. Chemical separation of the extract was conducted if information on the possible active secondary metabolites was not available. GC–MS analysis and stationary-phase HPLC found piperine to be abundant in the *P. amalago* var. *amalago* extract (Supplemental 2). Piperine exhibited similar inhibitory trends to that of the water extract (Table 3). The results suggest that piperine, a compound found commonly in *Piper* spp. [76, 80], with previously demonstrated insecticidal [30], synergistic [81], and larvicidal [77] properties, was the most likely secondary

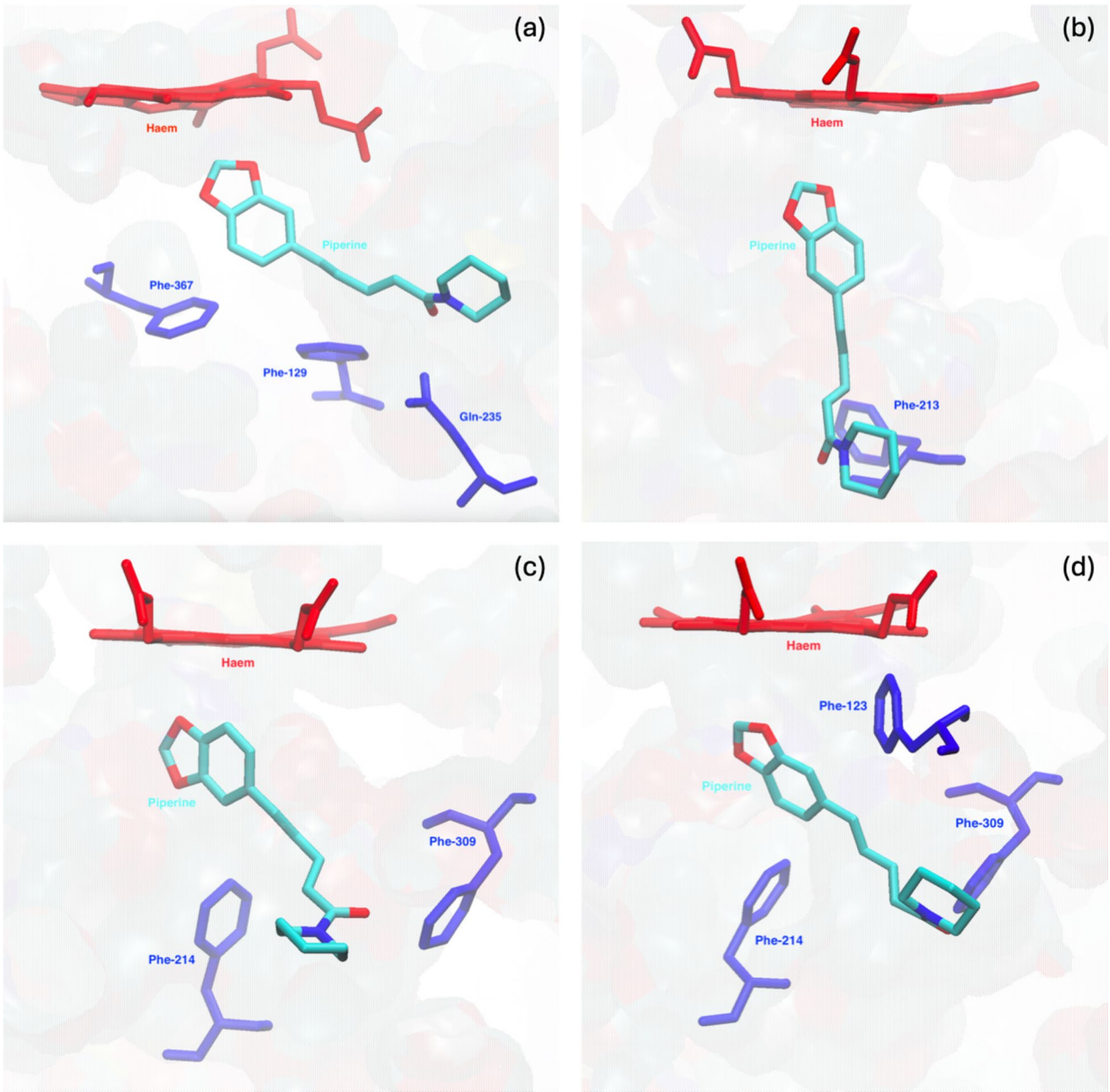

Fig. 7 Best theoretical binding pose achieved for *P. amalago* var. *amalago* compound. Piperine complexed with **a**, **b**, **c**, **d** CYPs 4G17, 6M2, 6P3, and 6P9a. CYPs are shown in surface representation (grey), with key residues identified for binding shown (blue) and the heme group (red) shown in stick representation. The ligand is also shown in stick representation, colored according to atom type (C—cyan; N—blue; O—red; H—white)

metabolite responsible for the CYP inhibitory property of the *P. amalago* var. *amalago* extract in vitro as well as the insecticidal activity of the extract against *An. gambiae* in this study.

Further in vivo studies found that *C. verticillata* demonstrated no insecticidal activity against the mosquitoes tested; however, the ethanolic extracts of *P. amalago amalago* and *K. pinnata* produced dose-dependent insecticidal activity against *An. gambiae* (Fig. 1). In order to identify genes that may play a protective role against the toxicity of the plant extracts, the effects on gene expression following exposure to sublethal doses of extracts (Figs. 3, 4, and Tables 4, 5) was assessed. The paired-end sequences following exposure of *An. gambiae* to a sublethal dosage of *P. amalago* var. *amalago* or *K. pinnata* could be mapped to a total of 13,797 genes, with good alignment obtained for both treatments (~88% and ~84%, respectively) and the solvent control

(~90%). Of these, 708 genes and 893 genes were differentially expressed, respectively, compared to the control. The enzymes that were upregulated following both plant extract treatments (Fig. 3 and Table 4) were likely involved in the metabolism of the compounds found in the plant extracts when applied topically. In contrast, the downregulation of trypsins, along with the upregulation of DNA-damage-inducible protein (Table 4), may indicate a move towards survival. Cuticular proteins, including CYP4G17, frequently overexpressed in resistant populations, are known to be involved in the oxidative decarbonylases that catalyze the final step in cuticular hydrocarbon synthesis [82, 83]; they were observed to be downregulated in relation to the control (Fig. 3), along with other cuticular proteins (Table 4). However, previous whole-genome transcription studies demonstrated differential upregulation of CYP4G17 along with the differential upregulation of other cuticular proteins in anopheline mosquitoes treated with insecticides [83].

RNA sequencing analysis for *An. funestus* following exposure to the ethanolic extract of *C. verticillata* was compared to *An. funestus* treated with ethanol only. The paired-end sequences could be mapped to a total of 14,177 genes. A similar pattern to the findings for *An. gambiae* could be observed, with a number of genes coding for enzymes being upregulated. In this study, similar CYP orthologs were similarly upregulated or downregulated across the treatments (Table 5). An overall limitation of the RNA sequencing analysis was the large number of genes for which no annotation was available; this was especially applicable to the *An. funestus* genome. As these genomes are further characterized, the number of differentially expressed genes coding for unspecified products may reveal new information describing the mechanism of action underlying the treatments applied. CYP6P9a was downregulated in *An. funestus* treated with *C. verticillata*, albeit not differentially. Its low toxicity in vivo may explain the limited differential expression (Table 5) of the known genes.

Following the in vitro and RNA sequencing results, in silico studies were conducted to ascertain binding affinity and possible interactions of the active ingredients within each extract with the CYP enzymes they were predicted to regulate. A common feature of the molecular docking results with the five active ingredients (piperine (identified in *P. amalago* var. *amalago;* Supplemental 2); 2,3-diacetoxytormentic acid [from *C. verticillata* previously identified in the extract [22]; bryophyllin A, bryophyllin C, and luteolin-7-*O*-β-D-glucoside (widely reported in an ethanol extract of *K. pinnata* [20])] on five CYP isoforms (4G17, 6M2, 6P3, and 9J3 from *An. gambiae*; 6P9a from *An. funestus*; selected on the basis of in vitro and RNA sequencing results) was the mediation of the ligands in their respective active sites by π–π stacking interactions with phenylalanine residues conserved across all eukaryotic CYP enzymes [84, 85]. These phenylalanine residues constitute key interaction points in substrate recognition sites surrounding the binding pocket. The molecular docking results revealed strong binding affinity by all compounds evaluated, with compounds from *K. pinnata* showing more specific activity toward CYP6P3 and CYP6M2 from *An. gambiae* (Table 6, Fig. 5), 2,3-diacetoxytormentic acid from *C. verticillata* showing specificity toward CYP6P9a from *An. funestus* (Fig. 6, Table 6), and piperine, showing broader activity toward all CYPs evaluated, with the exception of CYP9J3 (Table 6, Fig. 7). The results are similar to those obtained in vitro, demonstrating the likeliness of these compounds as active agents in the plant extracts.

With the exception of piperine and bryophillin A, CYP4G17 exhibited relatively low affinity toward the compounds evaluated in comparison to the other CYPs that were modelled. This may be a function of a differently shaped binding pocket to isoforms from the CYP6 and CYP9 families. Specifically, its active site is narrower and more elongated, which may confer some substrate specificity suited for long-chain insecticides commonly used on mosquitoes. This could explain its upregulation in the presence of insecticides [82, 83] but downregulation following treatment with *P. amalago* var. *amalago* and *K. pinnata*, which may be preferentially metabolized by isoforms from the CYP6 family.

Kalanchoe pinnata and *P. amalago amalago* were the only extracts to demonstrate dose-dependent toxicity towards anopheline mosquitoes by targeting key metabolic enzymes associated with insecticide resistance in these vectors. The observed in vitro and in silico results, as well as the toxicity towards *An. gambiae* supports the synergistic potential of these compounds. This synergistic effect is a result of the decreased availability of those key enzymes involved in the metabolism of insecticides, allowing the insecticide to reach its target site. The increase in the effectivity of permethrin, when used synergistically with *K. pinnata,* demonstrates this effect. Although synergistic studies were not conducted with *P. amalago amalago* on any anopheline mosquitoes in this study, a previous study demonstrated synergism of *P. amalago* var. *amalago* with pyrethroids on aedine mosquitoes [86]. Other studies have also demonstrated the synergistic activity of *Piper* spp. and the active metabolite piperine with pyrethroids [74, 76]. Piperine, the active metabolite in the *P. amalago amalago* extract, demonstrated strong binding affinity to all CYPs assessed in silico. Piperine's

broad-spectrum activity, as a function of its methylenedioxyphenyl group, enables it to bind to the active site of multiple CYPs responsible for metabolizing insecticides [29, 76, 79]. This makes it a strong candidate as a synergist. Its smaller, less decorated nature also makes it an ideal scaffold for further optimization as a single compound. On the other hand, the extract from *K. pinnata*, with more than one compound (bryophyllin A, bryophyllin C, and luteolin-7-*O*-β-D-glucoside) exhibiting very strong affinity for CYPs central to insecticide resistance, may be a suitable natural candidate in extract form to bypass this obstacle in large mosquito populations.

Conclusion

This study demonstrates that aqueous plant extracts that inhibit anopheline CYP, with IC_{50}s less than 6.95 µg/ml have the potential to be developed as synergists to increase the toxicity of insecticides used to manage mosquito populations. This synergistic activity is the result of the strong affinity, demonstrated in silico, of their secondary metabolites for CYP enzymes known to be upregulated in insecticide-resistant anopheline mosquito populations, as well as their demonstrated toxicity towards anopheline mosquitoes. The piperine compound (isolated from *P. amalago* var. *amalago*) and the *K. pinnata* extract were identified as ideal candidates for further development as insecticide synergists, to target mosquito vectors of malaria and other diseases.

Abbreviations

CYP	Cytochrome P450
GST	Glutathione *S*-transferase
CCE	Carboxy/cholinesterase
$NADP^+$	Nicotinamide adenine dinucleotide phosphate
DMSO	Dimethyl sulfoxide
DEF	Diethoxyfluorescein
K_m	Michaelis constant
PBO	Piperonyl butoxide
IC_{50}	The concentration that inhibits 50% enzyme activity
LD_{50}	Lethal dose that results in 50% mortality
var	Variety
RNA	Ribonucleic acid
RNA-seq	Ribonucleic acid sequence
spp.	Species

Supplementary Information

The online version contains supplementary material available at https://doi.org/10.1186/s12936-025-05254-4.

Supplementary Material 1: Structural drawing of compounds from the ethanolic plant extract. Piperine (a) from *P. amalago* var *amalago*; bryophyllin A (b), bryophyllin C (c) and luteolin-7-*O*-β-D-glucoside (d) from *K. pinnata* and 2,3-diacetoxytormentic acid (e) from *C. verticillata*.

Supplementary Material 2. Chromatograph of the (a) purified piperine and (b) ethanolic plant extract of P. amalago var amalago.

Supplementary Material 3. Mosquito toxicology bioassays for ethanol-based plant extracts.

Supplementary Material 4. Metasequence analysis of *An. funestus* treated with *Condea (Hyptis) verticillata* vs the ethanol control.

Supplementary Material 5. Metasequence analysis of *An. gambiae* treated with *Kalanchoe (Bryophyllum) pinnata* vs the ethanol control.

Supplementary Material 6. Metasequence analysis of *An. gambiae* treated with *Piper amalago var amalago* vs the ethanol control.

Acknowledgements

We are grateful to Dr. David Picking for technical assistance in the tea preparations, Chelsea Frank for technical support with the ethanol extract preparations and M.T. Babumon for support with the GC-MS and HPLC assays. We are also grateful for the support in data analysis by the project Research Infrastructures for the control of vector-borne diseases (Infravec2), which has received funding from the European Union's Horizon 2020 Research and Innovation Programme under grant agreement No. 731060.

Disclaimer

The views expressed in this manuscript are those of the authors and do not necessarily reflect the official policy or position of the Centers for Disease Control and Prevention.

Author contributions

Conceptualization: Sheena Francis, Audrey Lenhart, Mark J. I. Paine, Rupika Delgoda Data curation: Sheena Francis, William Irvine, Lucy Mackenzie-Impoinvil Formal analysis: Sheena Francis, William Irvine, Mark J. I. Paine, Rupika Delgoda Funding acquisition: Sheena Francis Investigation: Sheena Francis, William Irvine, Lucy Mackenzie-Impoinvil, Lucrecia Vizcaino, Rodolphe Poupardin Methodology: Sheena Francis, Audrey Lenhart, Mark J. I. Paine, Rupika Delgoda Writing: Sheena Francis, Lucy Mackenzie-Impoinvil, William Irvine Writing review and editing: Sheena Francis, William Irvine, Mark J. I. Paine, Rupika Delgoda, Audrey Lenhart.

Funding

This research was financially supported by the New Initiatives Grant University of the West Indies, Jamaica [Grant number 16095P]; Bursaries received from the Staff Development fund, University of Technology, Jamaica and the CARISCIENCE, Trinidad.

Availability of data and materials

Data is provided within the manuscript or as supplementary information files.

Declarations

Competing interests

The authors declare no competing interests.

Author details

[1]Caribbean Centre for Research in Biosciences, Natural Products Institute, University of the West Indies, Kingston, Jamaica. [2]The Mosquito Control Research Unit, University of the West Indies, Kingston, Jamaica. [3]Entomology Branch, Division of Parasitic Diseases and Malaria, National Center for Emerging and Zoonotic Infectious Diseases, Centers for Disease Control and Prevention, 1600 Clifton Rd, Atlanta, GA 30329, USA. [4]Cell Therapy Institute, Paracelsus Medical University, Salzburg, Austria. [5]Vector Group, Liverpool School of Tropical Medicine, Liverpool, UK.

Received: 16 October 2024 Accepted: 11 January 2025
Published online: 22 January 2025

References

1. WHO. World malaria report 2023. Geneva: World Health Organization; 2023.

2. Ryan SJ, Lippi CA, Zermoglio F. Shifting transmission risk for malaria in Africa with climate change: a framework for planning and intervention. Malar J. 2020;19:170.
3. Woyessa D, Morou E, Wipf N, Dada N, Mavridis K, Vontas J, et al. Species composition, infection rate and detection of resistant alleles in *Anopheles funestus* (Diptera: Culicidae) from Lare, a malaria hotspot district of Ethiopia. Malar J. 2023;22:233.
4. Kusimo MO, Mackenzie-Impoinvil L, Ibrahim SS, Muhammad A, Irving H, Hearn J, et al. Pyrethroid resistance in the New World malaria vector *Anopheles albimanus* is mediated by cytochrome P450 CYP6P5. Pestic Biochem Physiol. 2022;183:105061.
5. David JP, Ismail HM, Chandor-Proust A, Paine MJ. Role of cytochrome P450s in insecticide resistance: impact on the control of mosquito-borne diseases and use of insecticides on Earth. Philos Trans R Soc Lond B Biol Sci. 2013;368:20120429.
6. Nauen R, Bass C, Feyereisen R, Vontas J. The role of cytochrome P450s in insect toxicology and resistance. Annu Rev Entomol. 2022;67:105–24.
7. Matowo J, Weetman D, Pignatelli P, Wright A, Charlwood JD, Kaaya R, et al. Expression of pyrethroid metabolizing P450 enzymes characterizes highly resistant *Anopheles* vector species targeted by successful deployment of PBO-treated bednets in Tanzania. PLoS ONE. 2022;17: e0249440.
8. WHO, Global Malaria Programme. Conditions for deployment of mosquito nets treated with a pyrethroid and piperonyl butoxide. Geneva: World Health Organization; 2017.
9. Gleave K, Lissenden N, Chaplin M, Choi L, Ranson H. Piperonyl butoxide (PBO) combined with pyrethroids in insecticide-treated nets to prevent malaria in Africa. Cochrane Database Syst Rev. 2021;5: CD012776.
10. Maiteki-Sebuguzi C, Gonahasa S, Kamya M, Katureebe A, Bagala I, Lynd A, et al. Effect of long-lasting insecticidal nets with and without piperonyl butoxide on malaria indicators in Uganda (LLINEUP): final results of a cluster-randomised trial embedded in a national distribution campaign. Lancet Infect Dis. 2023;23:247–58.
11. Francis S, Shields M, Jacobs H, Delgoda R. In-vitro assessment of chromones, alkaloids and other natural products from Caribbean plants as potential anti-tuberculars and chemopreventors. In: Goncalves R, Pinto M, editors. Natural products: structure, bioactivity and applications. New York: Nova Publishers; 2012.
12. Francis S, Laurieri N, Nwokocha C, Delgoda R. Treatment of rats with apocynin has considerable inhibitory effects on arylamine N-acetyltransferase activity in the liver. Sci Rep. 2016;6:26906.
13. Riveron JM, Irving H, Ndula M, Barnes KG, Ibrahim SS, Paine MJ, et al. Directionally selected cytochrome P450 alleles are driving the spread of pyrethroid resistance in the major malaria vector *Anopheles funestus*. Proc Natl Acad Sci USA. 2013;110:252–7.
14. Muller P, Warr E, Stevenson BJ, Pignatelli PM, Morgan JC, Steven A, et al. Field-caught permethrin-resistant *Anopheles gambiae* overexpress CYP6P3, a P450 that metabolises pyrethroids. PLoS Genet. 2008;4: e1000286.
15. Stevenson BJ, Bibby J, Pignatelli P, Muangnoicharoen S, O'Neill PM, Lian LY, et al. Cytochrome P450 6M2 from the malaria vector *Anopheles gambiae* metabolizes pyrethroids: sequential metabolism of deltamethrin revealed. Insect Biochem Mol Biol. 2011;41:492–502.
16. Yunta C, Hemmings K, Stevenson B, Koekemoer LL, Matambo T, Pignatelli P, et al. Cross-resistance profiles of malaria mosquito P450s associated with pyrethroid resistance against WHO insecticides. Pestic Biochem Physiol. 2019;161:61–7.
17. Yunta C, Ooi JMF, Oladepo F, Grafanaki S, Pergantis SA, Tsakireli D, et al. Chlorfenapyr metabolism by mosquito P450s associated with pyrethroid resistance identifies potential activation markers. Sci Rep. 2023;13:14124.
18. Lees RS, Ismail HM, Logan RAE, Malone D, Davies R, Anthousi A, et al. New insecticide screening platforms indicate that Mitochondrial Complex I inhibitors are susceptible to cross-resistance by mosquito P450s that metabolise pyrethroids. Sci Rep. 2020;10:16232.
19. Biggs DA, Porter RB, Reynolds WF, Williams LA. A new hyptadienic acid derivative from *Hyptis verticillata* (Jacq.) with insecticidal activity. Nat Prod Commun. 2008;3:1934578X0800301104.
20. Supratman U, Fujita T, Akiyama K, Hayashi H. New insecticidal bufadienolides, Bryophyllin C, from *Kalanchoe pinnata*. Biosci Biotechnol Biochem. 2000;64:1310–2.
21. Jacobs H, Seeram NP, Nair MG, Reynolds WF, Stewart M. Amides of *Piper amalago* var. *nigrinodum*. J Indian Chem Soc. 1999;76:713–8.
22. Picking D, Chambers B, Barker J, Shah I, Porter R, Naughton DP, et al. Inhibition of cytochrome P450 activities by extracts of *Hyptis verticillata* Jacq.: assessment for potential herb-drug interactions. Molecules. 2018;23:430.
23. Shields M, Niazi U, Badal S, Yee T, Sutcliffe MJ, Delgoda R. Inhibition of CYP1A1 by Quassinoids found in *Picrasma excelsa*. Planta Med. 2009;75:137–41.
24. Shields M. The effect of Jamaican medicinal plants on the activities of cytochrome P450 enzymes [MPhil]. Jamaica: University of the West Indies; 2006.
25. Picking D, Delgoda R, Younger N, Germosen-Robineau L, Boulogne I, Mitchell S. TRAMIL ethnomedicinal survey in Jamaica. J Ethnopharmacol. 2015;169:314–27.
26. Murray J, Picking D, Lamm A, McKenzie J, Hartley S, Watson C, et al. Significant inhibitory impact of dibenzyl trisulfide and extracts of *Petiveria alliacea* on the activities of major drug-metabolizing enzymes in vitro: an assessment of the potential for medicinal plant-drug interactions. Fitoterapia. 2016;111:138–46.
27. Wauchope S, Roy MA, Irvine W, Morrison I, Brantley E, Gossell-Williams M, et al. Dibenzyl trisulfide binds to and competitively inhibits the cytochrome P450 1A1 active site without impacting the expression of the aryl hydrocarbon receptor. Toxicol Appl Pharmacol. 2021;419:115502.
28. McNeil MJ, Porter RBR, Rainford L, Dunbar O, Francis S, Laurieri N, et al. Chemical composition and biological activities of the essential oil from *Cleome rutidosperma* DC. Fitoterapia. 2018;129:191–7.
29. Murray M. Toxicological actions of plant-derived and anthropogenic methylenedioxyphenyl-substituted chemicals in mammals and insects. J Toxicol Environ Health. 2012;15:365–95.
30. Durofil A, Radice M, Blanco-Salas J, Ruiz-Tellez T. *Piper aduncum* essential oil: a promising insecticide, acaricide and antiparasitic: a review. Parasite. 2021;28:42.
31. Gainza YA, Fantatto RR, Chaves FC, Bizzo HR, Esteves SN, Chagas AC. *Piper aduncum* against *Haemonchus contortus* isolates: cross resistance and the research of natural bioactive compounds. Rev Bras Parasitol Vet. 2016;25:383–93.
32. Jensen HR, Scott IM, Sims S, Trudeau VL, Arnason JT. Gene expression profiles of *Drosophila melanogaster* exposed to an insecticidal extract of *Piper nigrum*. J Agric Food Chem. 2006;54:1289–95.
33. Francis SA, Taylor-Wells J, Gross AD, Bloomquist JR. Toxicity and physiological actions of carbonic anhydrase inhibitors to *Aedes aegypti* and *Drosophila melanogaster*. Insects. 2016;8:2.
34. Brogdon WG, McAllister JC. Insecticide resistance and vector control. Emerg Infect Dis. 1998;4:605–13.
35. James MM, Troy DA, Derek TC, Aaron DG, Daniel RS, Fan T, et al. Carbamate and pyrethroid resistance in the akron strain of *Anopheles gambiae*. Pestic Biochem Physiol. 2015;121:116–21.
36. Andrews S, Krueger F, Segonds-Pichon A, Biggins L, Krueger C, Wingett S. FastQC: a quality control tool for high throughput sequence data. 2010. p. 370. http://www.bioinformatics.babraham.ac.uk/projects/fastqc. Accessed 31 Oct 2022.
37. Bolger AM, Lohse M, Usadel B. Trimmomatic: a flexible trimmer for Illumina sequence data. Bioinformatics. 2014;30:2114–20.
38. Holt RA, Subramanian GM, Halpern A, Sutton GG, Charlab R, Nusskern DR, et al. The genome sequence of the malaria mosquito *Anopheles gambiae*. Science. 2002;298:129–49.
39. Ayala D, Akone-Ella O, Kengne P, Johnson H, Heaton H, Collins J, et al. The genome sequence of the malaria mosquito, *Anopheles funestus*, Giles, 1900. Wellcome Open Res. 2022;7:287.
40. Kim D, Paggi JM, Park C, Bennett C, Salzberg SL. Graph-based genome alignment and genotyping with HISAT2 and HISAT-genotype. Nat Biotechnol. 2019;37:907–15.
41. Danecek P, Bonfield JK, Liddle J, Marshall J, Ohan V, Pollard MO, et al. Twelve years of SAMtools and BCFtools. Gigascience. 2021;10: giab008.
42. Anders S, Pyl PT, Huber W. HTSeq—a Python framework to work with high-throughput sequencing data. Bioinformatics. 2015;31:166–9.
43. RStudio Team. RStudio: integrated development for R. Boston: Rstudio Team, PBC; 2020.
44. Love MI, Huber W, Anders S. Moderated estimation of fold change and dispersion for RNA-seq data with DESeq2. Genome Biol. 2014;15:550.
45. Thomas PD, Ebert D, Muruganujan A, Mushayahama T, Albou LP, Mi H. Panther: making genome-scale phylogenetics accessible to all. Protein Sci. 2022;31:8–22.

46. Turner P. XMGRACE, Version 5.1. 19. Center for Coastal and Land-Margin Research, Oregon Graduate Institute of Science and Technology, Beaverton, OR. 2005;2.
47. Jumper J, Evans R, Pritzel A, Green T, Figurnov M, Ronneberger O, et al. Highly accurate protein structure prediction with AlphaFold. Nature. 2021;596:583–9.
48. Giraldo-Calderon GI, Emrich SJ, MacCallum RM, Maslen G, Dialynas E, Topalis P, et al. VectorBase: an updated bioinformatics resource for invertebrate vectors and other organisms related with human diseases. Nucleic Acids Res. 2015;43(Database):D707–13.
49. Samuels ER, Sevrioukova I. Structure-Activity Relationships of rationally designed ritonavir analogues: impact of side-group stereochemistry, headgroup spacing, and backbone composition on the interaction with CYP3A4. Biochemistry. 2019;58:2077–87.
50. Berendsen HJ, van der Spoel D, van Drunen R. GROMACS: a message-passing parallel molecular dynamics implementation. Comput Phys Commun. 1995;91:43–56.
51. Vanommeslaeghe K, Hatcher E, Acharya C, Kundu S, Zhong S, Shim J, et al. CHARMM general force field: a force field for drug-like molecules compatible with the CHARMM all-atom additive biological force fields. J Comput Chem. 2010;31:671–90.
52. Berendsen HJ, Grigera JR, Straatsma TP. The missing term in effective pair potentials. J Phys Chem. 1987;91:6269–71.
53. Berendsen HJ, Postma J, van Gunsteren WF, DiNola A, Haak JR. Molecular dynamics with coupling to an external bath. J Chem Phys. 1984;81:3684–90.
54. Parrinello M, Rahman A. Polymorphic transitions in single crystals: a new molecular dynamics method. J Appl Phys. 1981;52:7182–90.
55. Hess B, Bekker H, Berendsen HJ, Fraaije JG. LINCS: a linear constraint solver for molecular simulations. J Comput Chem. 1997;18:1463–72.
56. Páll S, Hess B. A flexible algorithm for calculating pair interactions on SIMD architectures. Comput Phys Commun. 2013;184:2641–50.
57. Essmann U, Perera L, Berkowitz ML, Darden T, Lee H, Pedersen LG. A smooth particle mesh Ewald method. J Chem Phys. 1995;103:8577–93.
58. Morris GM, Huey R, Lindstrom W, Sanner MF, Belew RK, Goodsell DS, et al. AutoDock4 and AutoDockTools4: automated docking with selective receptor flexibility. J Comput Chem. 2009;30:2785–91.
59. Hanwell MD, Curtis DE, Lonie DC, Vandermeersch T, Zurek E, Hutchison GR. Avogadro: an advanced semantic chemical editor, visualization, and analysis platform. J Cheminform. 2012;4:1–17.
60. Trott O, Olson AJ. AutoDock Vina: improving the speed and accuracy of docking with a new scoring function, efficient optimization, and multithreading. J Comput Chem. 2010;31:455–61.
61. Humphrey W, Dalke A, Schulten K. VMD: visual molecular dynamics. J Mol Gr. 1996;14:33–8.
62. Laskowski RA, Swindells MB. LigPlot+: multiple ligand–protein interaction diagrams for drug discovery. Washington: ACS Publications; 2011.
63. Abbott WS. A method of computing the effectiveness of an insecticide. J Econ Entomol. 1925;18:265–7.
64. Edi CV, Djogbenou L, Jenkins AM, Regna K, Muskavitch MA, Poupardin R, et al. CYP6 P450 enzymes and ACE-1 duplication produce extreme and multiple insecticide resistance in the malaria mosquito *Anopheles gambiae*. PLoS Genet. 2014;10: e1004236.
65. Krippendorff BF, Lienau P, Reichel A, Huisinga W. Optimizing classification of drug-drug interaction potential for CYP450 isoenzyme inhibition assays in early drug discovery. J Biomol Screen. 2007;12:92–9.
66. Wong FKA, Zheng EJ, Stärk H, Manson AL, Earl AM, Jaakkola T, Collins JJ. Benchmarking AlphaFold-enabled molecular docking predictions for antibiotic discovery. Mol Syst Biol. 2022;18: e11081.
67. Smith RD, Clark JJ, Ahmed A, Orban ZJ, Dunbar JB, Carlson HA. Updates to binding MOAD (Mother of All Databases): polypharmacology tools and their utility in drug repurposing. J Mol Biol. 2019;431:2423–33.
68. Kawasaki Y, Freire E. Finding a better path to drug selectivity. Drug Discov Today. 2011;16:985–90.
69. Koul SK, Taneja SC, Pushpangadan P, Dhar KL. Lignans of *Piper trichostachyon*. Phytochemistry. 1988;27:1479–82.
70. Burke B, Nair M. Phenylpropene, benzoic acid and flavonoid derivatives from fruits of Jamaican *Piper* species. Phytochemistry. 1986;25:1427–30.
71. Seeram NP, Lewis PA, Jacobs H, McLean S, Reynolds WF, Tay L-L, et al. 3,4-Epoxy-8,9-dihydropiplartine: a new imide from *Piper verrucosum*. J Nat Prod. 1996;59:436–7.
72. Nakajima M, Suzuki M, Yamaji R, Takashina H, Shimada N, Yamazaki H, et al. Isoform selective inhibition and inactivation of human cytochrome P450s by methylenedioxyphenyl compounds. Xenobiotica. 1999;29:1191–202.
73. Belzile A-S, Majerus SL, Podeszfinski C, Guillet G, Durst T, Arnason JT. Dillapiol derivatives as synergists: structure–activity relationship analysis. Pestic Biochem Physiol. 2000;66:33–40.
74. Jensen H, Scott I, Sims S, Trudeau V, Arnason J. The effect of a synergistic concentration of a *Piper nigrum* extract used in conjunction with pyrethrum upon gene expression in *Drosophila melanogaster*. Insect Mol Biol. 2006;15:329–39.
75. Pethuan S, Duangkaew P, Sarapusit S, Srisook E, Rongnoparut P. Inhibition against mosquito cytochrome P450 enzymes by rhinacanthin-A,-B, and-C elicits synergism on cypermethrin cytotoxicity in *Spodoptera frugiperda* cells. J Med Entomol. 2012;49:993–1000.
76. Scott IM, Jensen HR, Philogène BJ, Arnason JT. A review of *Piper* spp. (Piperaceae) phytochemistry, insecticidal activity and mode of action. Phytochem Rev. 2008;7:65–75.
77. Nair MG, Mansingh AP, Burke BA. Insecticidal properties of some metabolites of Jamaican *Piper* spp., and the amides synthesized from 5, 6-Z and E-butenolides of *Piper fadyenii*. Agric Biol Chem. 1986;50:3053–8.
78. Yee TH, Watson CT, Garraway E, Robinson D, Chisholm NNSG. Method and Products for Reducing the Population size of *Papilla demoleus L*. (Papilionidae). Jamaica. University of the West Indies. 2014.
79. Prill EA. Methylenedioxyphenyl compound as insecticide, insect repellent, and pyrethrin synergist. Boyce Thompson Institute for Plant Research Inc. USA1950.
80. Salehi B, Zakaria ZA, Gyawali R, Ibrahim SA, Rajkovic J, Shinwari ZK, et al. *Piper* species: a comprehensive review on their phytochemistry, biological activities and applications. Molecules. 2019;24:1364.
81. Dyer LA, Dodson CD, Stireman JO 3rd, Tobler MA, Smilanich AM, Fincher RM, et al. Synergistic effects of three *Piper* amides on generalist and specialist herbivores. J Chem Ecol. 2003;29:2499–514.
82. Balabanidou V, Kampouraki A, MacLean M, Blomquist GJ, Tittiger C, Juarez MP, et al. Cytochrome P450 associated with insecticide resistance catalyzes cuticular hydrocarbon production in *Anopheles gambiae*. Proc Natl Acad Sci USA. 2016;113:9268–73.
83. Messenger LA, Impoinvil LM, Derilus D, Yewhalaw D, Irish S, Lenhart A. A whole transcriptomic approach provides novel insights into the molecular basis of organophosphate and pyrethroid resistance in *Anopheles arabiensis* from Ethiopia. Insect Biochem Mol Biol. 2021;139:103655.
84. Dutkiewicz Z, Mikstacka R. Structure-based drug design for cytochrome P450 family 1 inhibitors. Bioinorg Chem Appl. 2018;2018:3924608.
85. Clarke N, Irvine W. In silico design and SAR study of dibenzyl trisulfide analogues for improved CYP1A1 inhibition. ChemistryOpen. 2022;11: e202200016.
86. Frank C. Exploration of the use of extracts of *Piper amalago* var *amalago* in the control of resistant Kingston and St. Andrew *Aedes aegypti* mosquitoes [M.Phil]. Jamaica: University of the West Indies Press; 2024.

Publisher's Note